



Argonne
NATIONAL
LABORATORY

... for a brighter future



U.S. Department
of Energy



A U.S. Department of Energy laboratory
managed by The University of Chicago

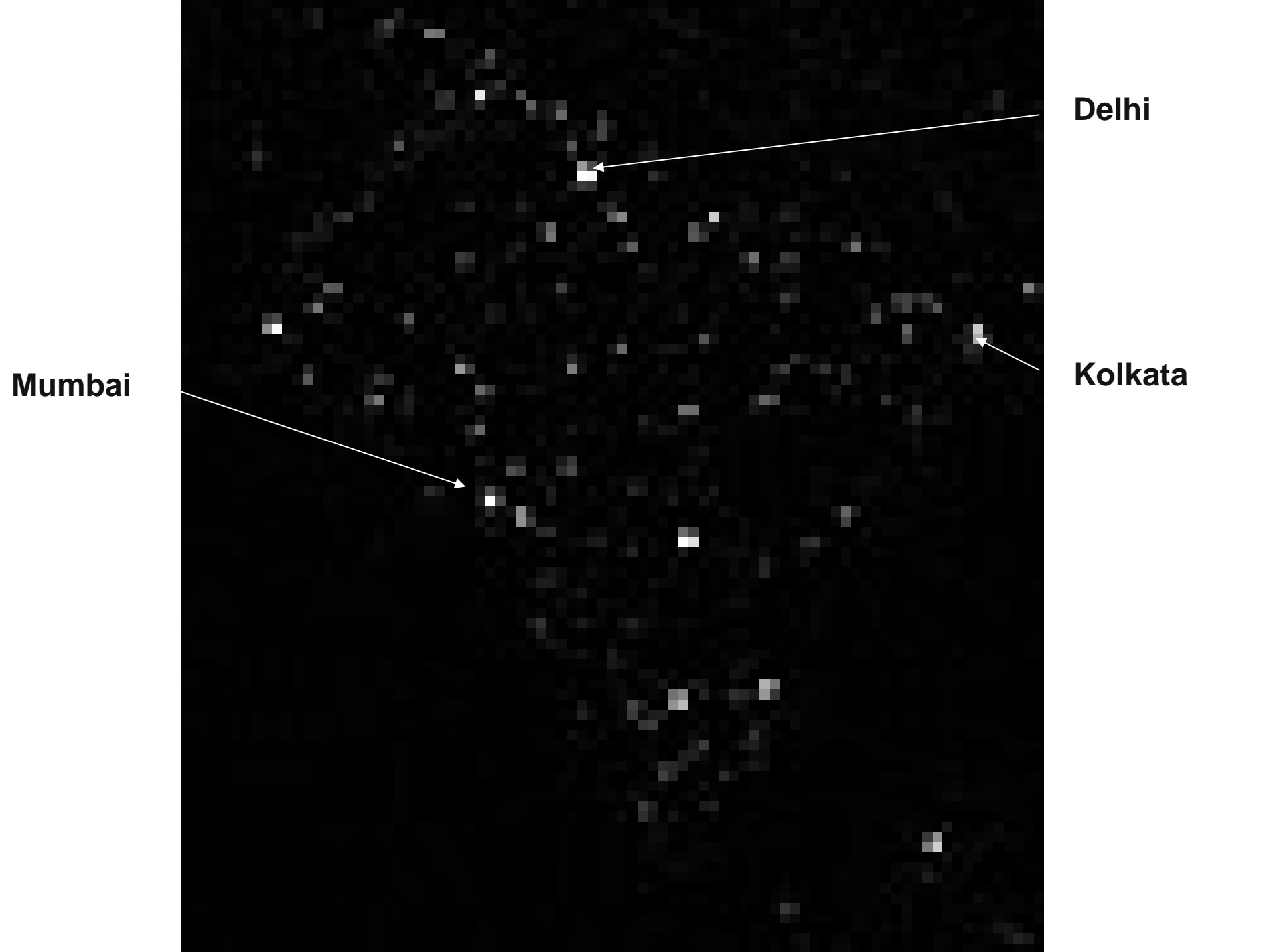
Detectors for Nuclear Astrophysics Experiments.

K.E. Rehm,

**Argonne National Laboratory,
Physics Division**



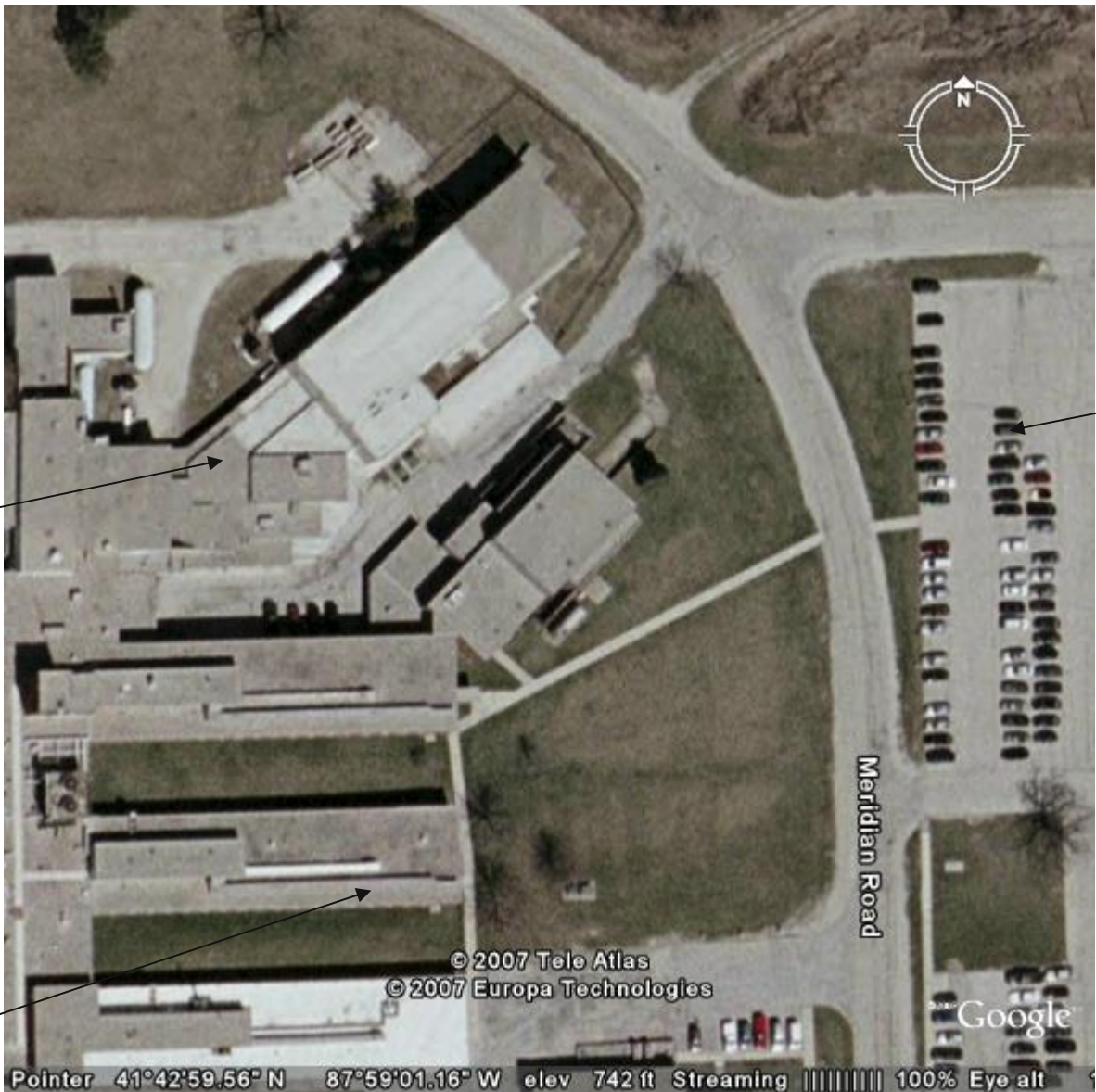
**Where were you on
November 13, 2007?
(Rosetta Mission (ESA))**



Delhi

Kolkata

Mumbai



**ATLAS
accelerator**

my car

my office

Example of nuclear reactions: CNO cycle

T = 10 million deg. T = 100 million deg.

	t = 4.3 × 10 ⁹ years	12.9 min
	+ 14.3 min	+ 14.3 min
	+ 1.1 × 10 ⁹ years	+ 3.2 min
	+ 2.1 × 10 ¹² years	+ 3.2 hrs
	+ 2.9 min	+ 2.9 min
	+ 2.0 × 10 ⁸ years	0.26 sec

$^{12}\text{C}(p, \gamma)^{13}\text{N}$: γ , charged particle

$^{13}\text{N} \rightarrow e^+ + \nu + ^{13}\text{C}$: ν , e^+ , charged part.

$^{13}\text{C}(p, \gamma)^{14}\text{N}$: γ , charged particle

$^{14}\text{N}(p, \gamma)^{15}\text{O}$: γ , charged particle

$^{15}\text{O} \rightarrow e^+ + \nu + ^{15}\text{N}$: ν , e^+ , charged part.

$^{15}\text{N}(p, \alpha)^{12}\text{C}$: α , charged particle

Many different detectors:

- Gamma detector arrays
- X-ray detectors
- Neutron detectors
- Neutrino detectors
- Charged particle detectors**

Ideal Detector

- Excellent energy (wave length) resolution
- Excellent time resolution
- High detection efficiency (large area)
- High count rate capability
- Stable over long running times
- No (low) backgrounds
- Low cost
- Long life time
- Easy to repair

Outline:

Silicon surface barrier detector (commercial products)

Gas-filled ionization chambers (built individually)

Magnetic Spectrometer (designed indiv., built commerc.)

Recoil separators (lecture II) (designed indiv., built commerc.)

Two options of charged-particle reactions:

- Light particle (p) on heavy target (^{22}Ne).

example: $^{22}\text{Ne}(p,\alpha)^{19}\text{F}$

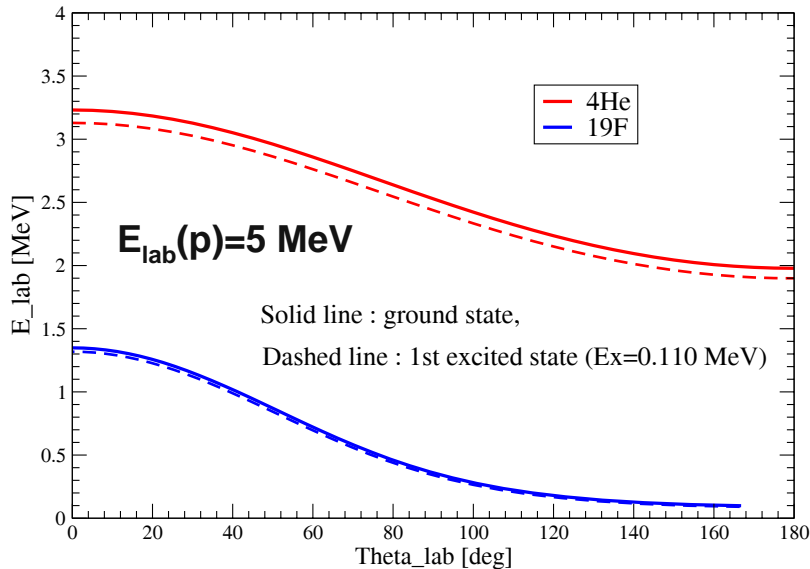
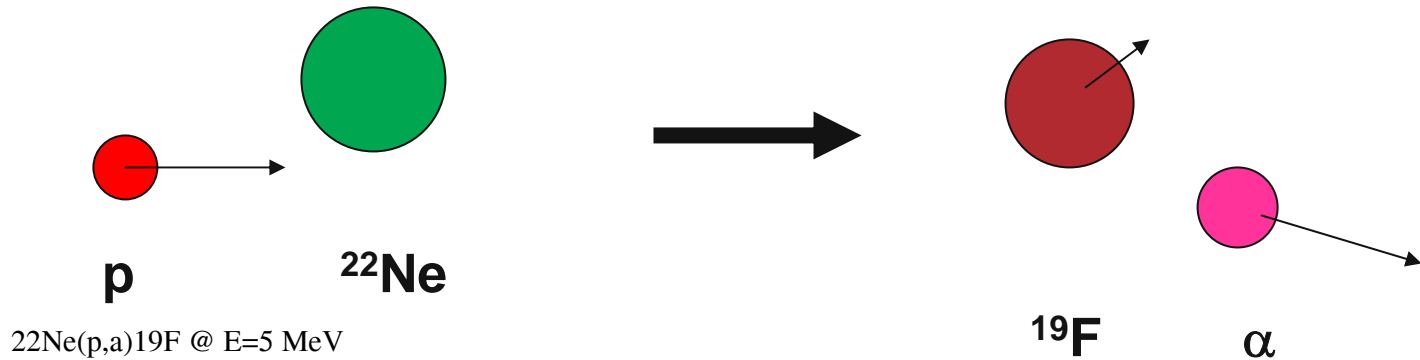
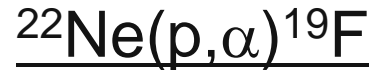
“normal kinematics”

- Heavy particle (^{22}Ne) on light target (p).

example: $p(^{22}\text{Ne},\alpha)^{19}\text{F}$

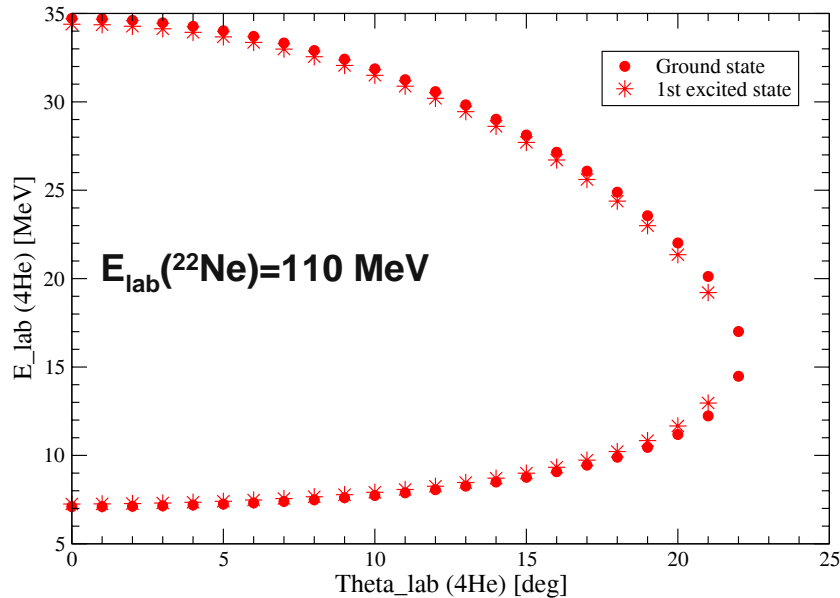
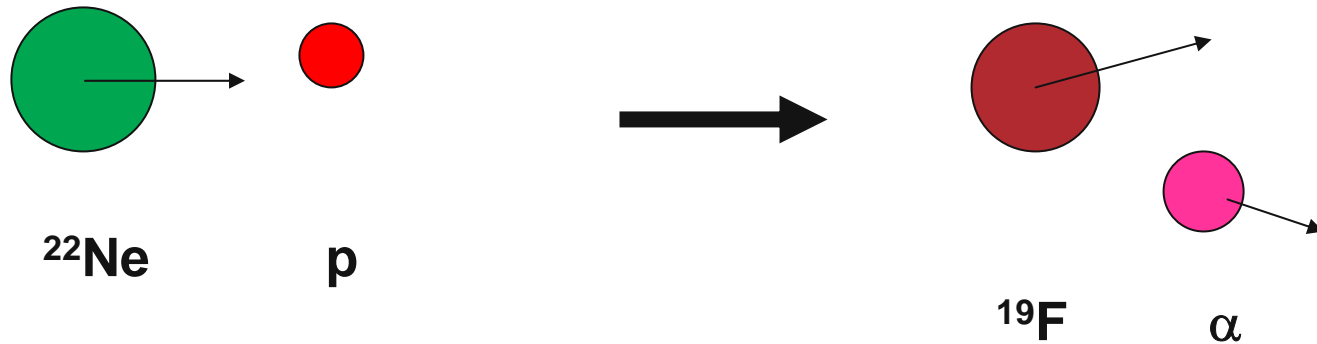
“inverse kinematics”

Normal kinematics



- Alphas cover all angles (0-180°)
- Alphas have most of the energy
- ¹⁹F has low energy
- Only possible for stable targets

Inverse kinematics

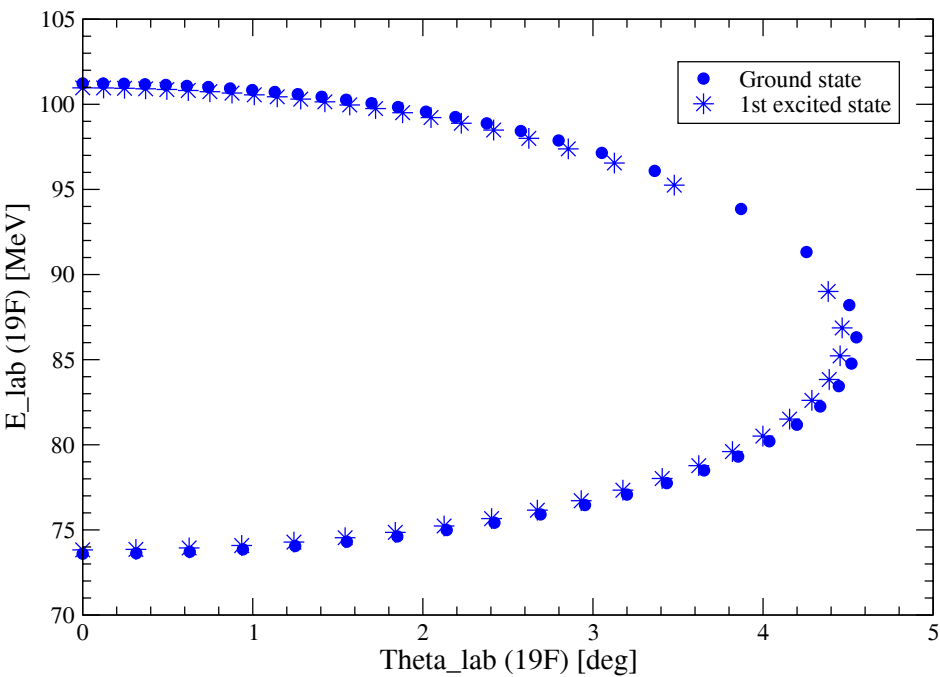
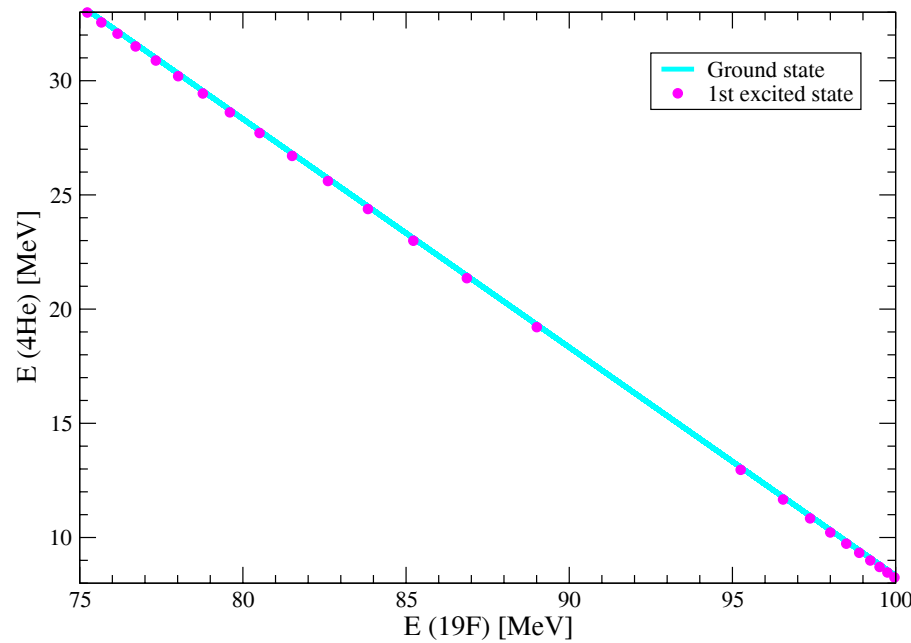
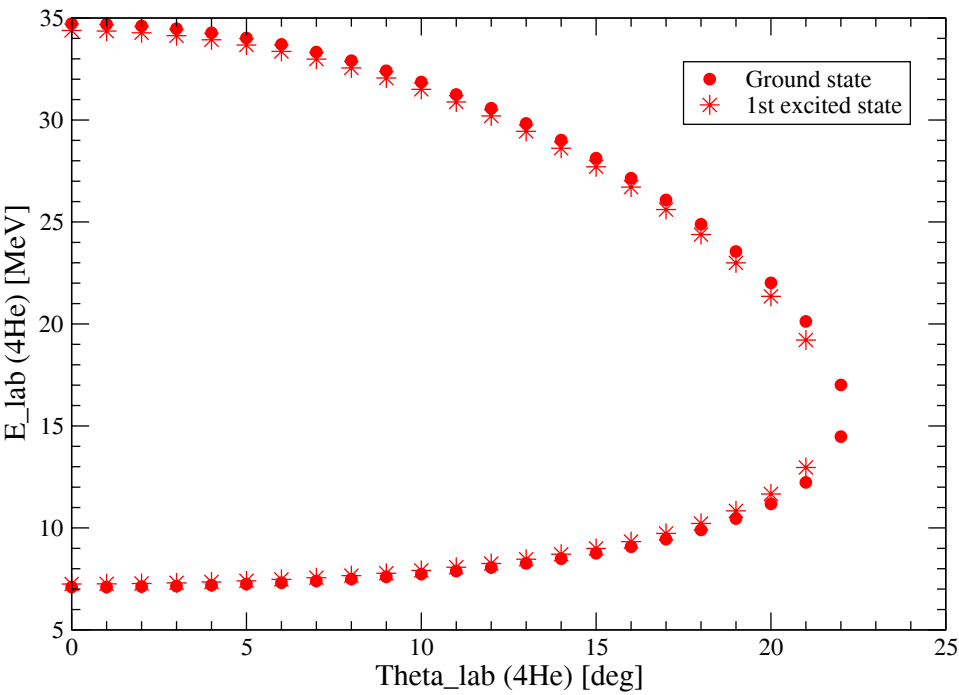


- ^{19}F and α 's are emitted forward
- ^{19}F and α share the energy
- possible for short-lived particles
- High ^{19}F energy good for identification

0

10

20 ϑ_{lab}

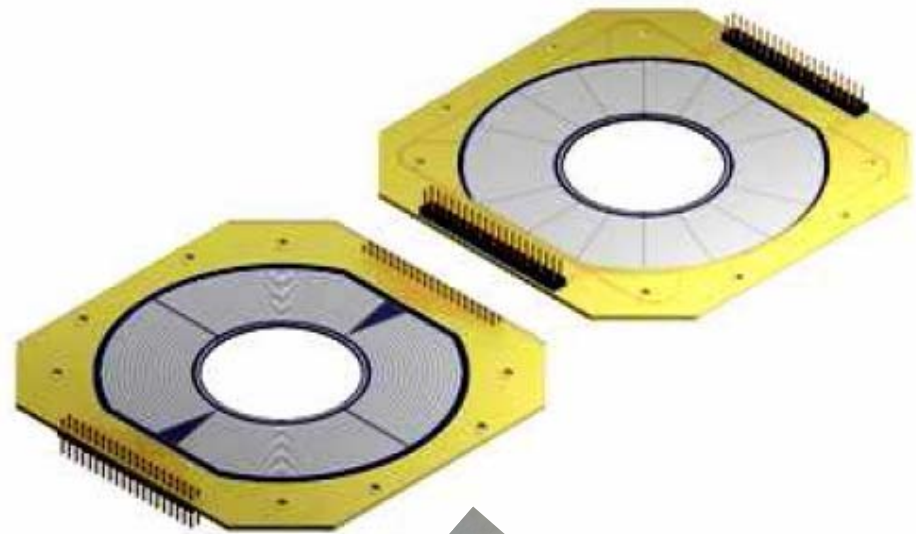


Inverse kinematics:

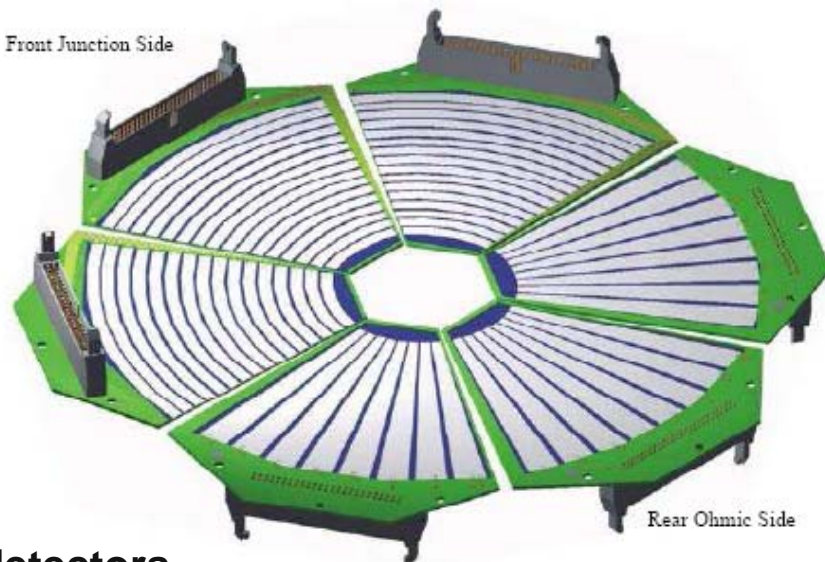
Much higher energies, but

Kinematic lines very close together

Geometry (e.g. beam spot) critical

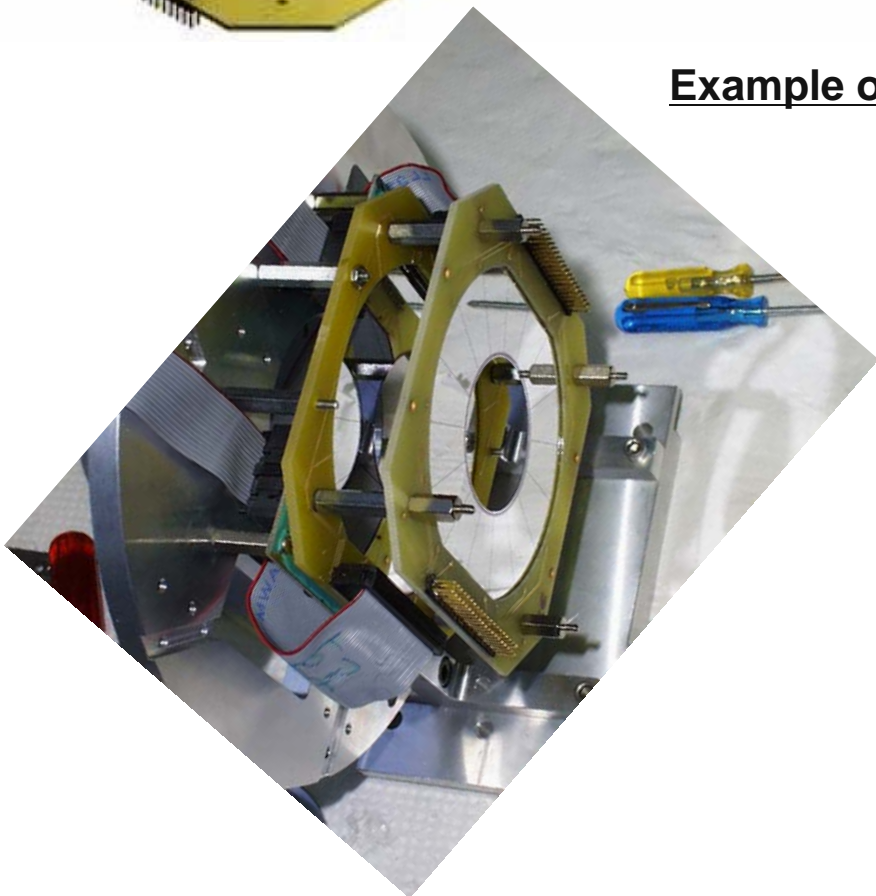


Front Junction Side



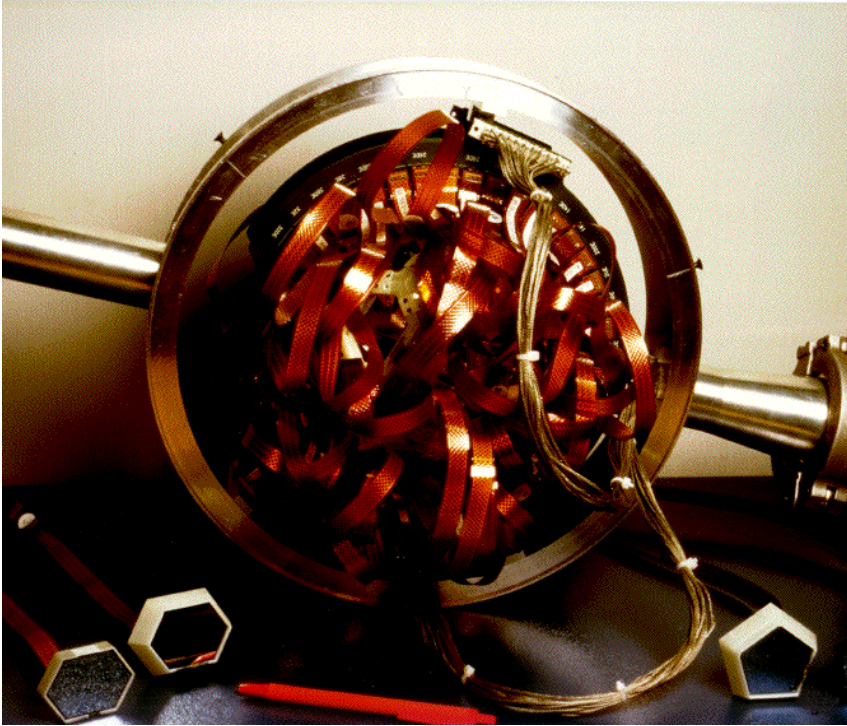
Rear Ohmic Side

Example of Si detectors

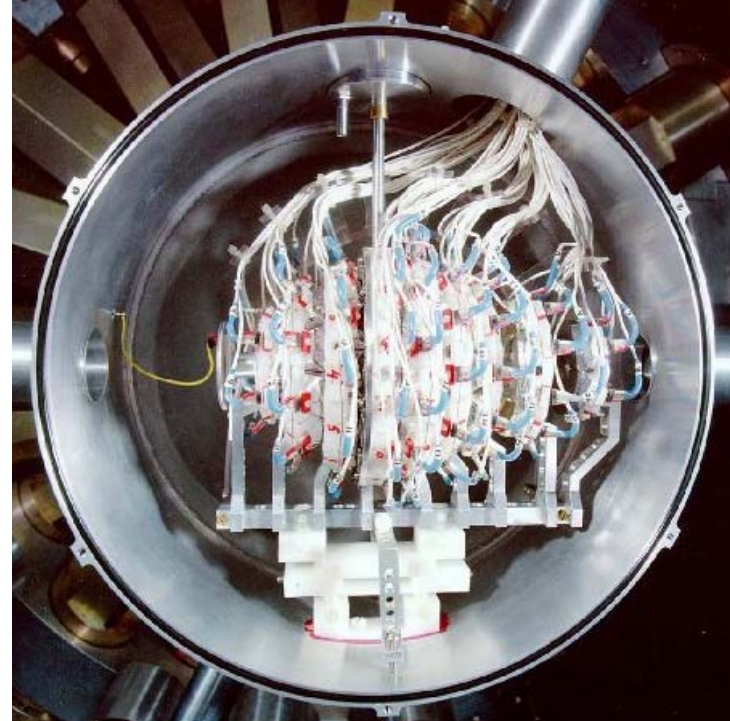


Particle Detector Arrays

(coincidence exp., particle transfer studies)

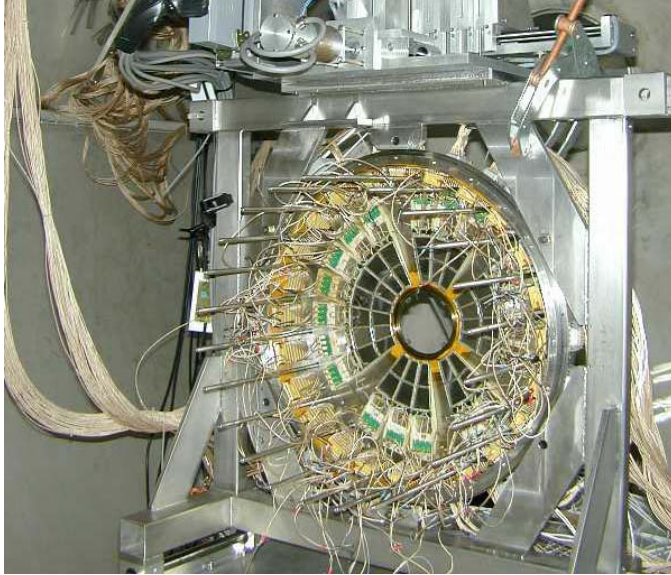


(Legnaro)



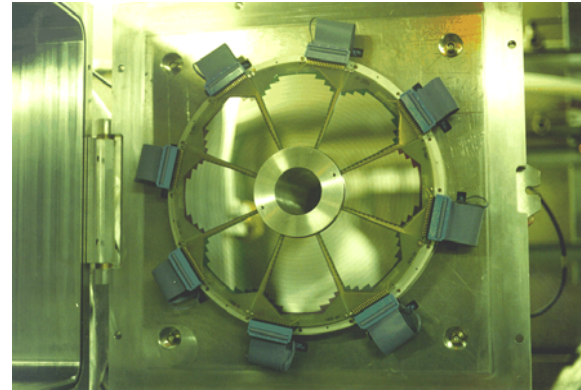
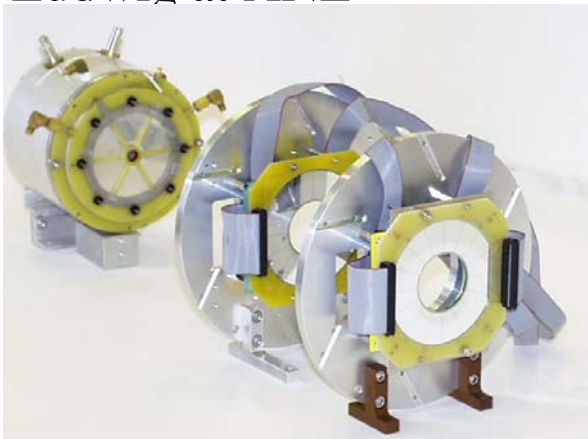
Microball

Particle Detectors

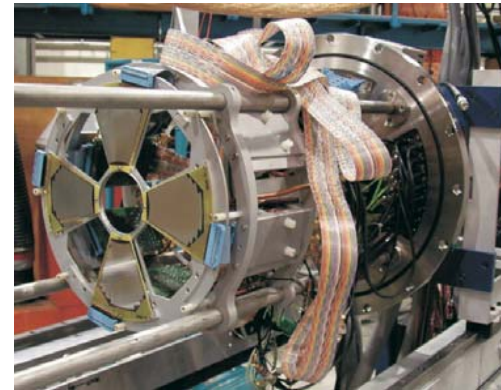


Garfield at Legnaro

Ludwig at ANL



LEDA at Louvain-la-Neuve

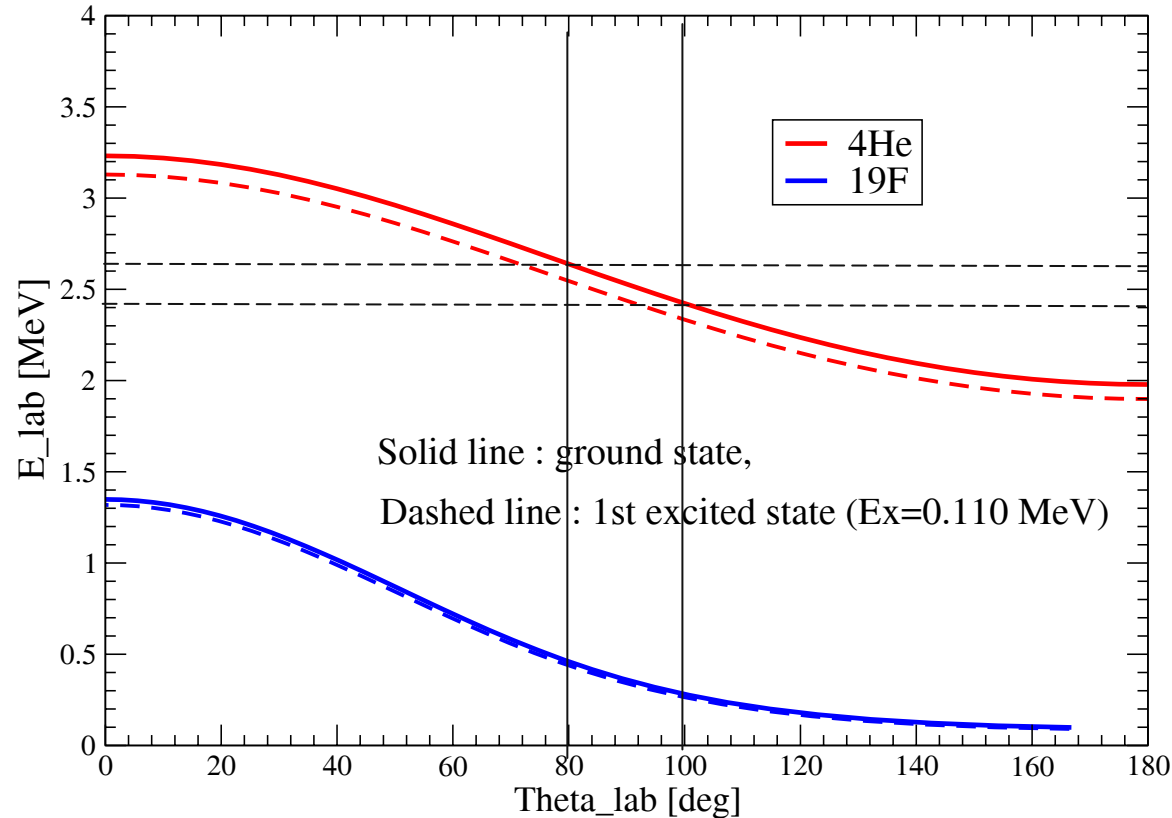


TUDA at TRIUMF ISAC

A few hundred channels
of electronics

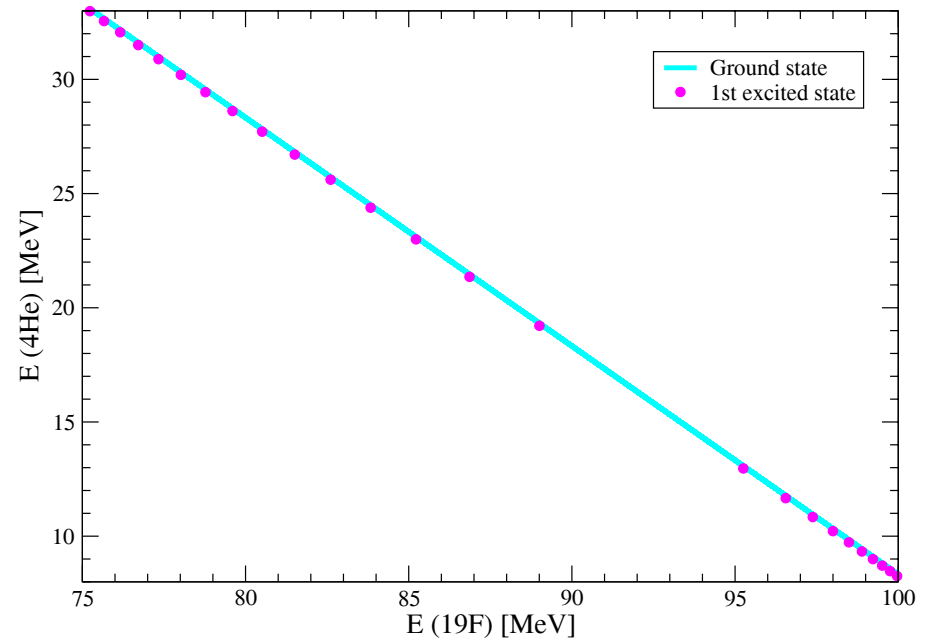
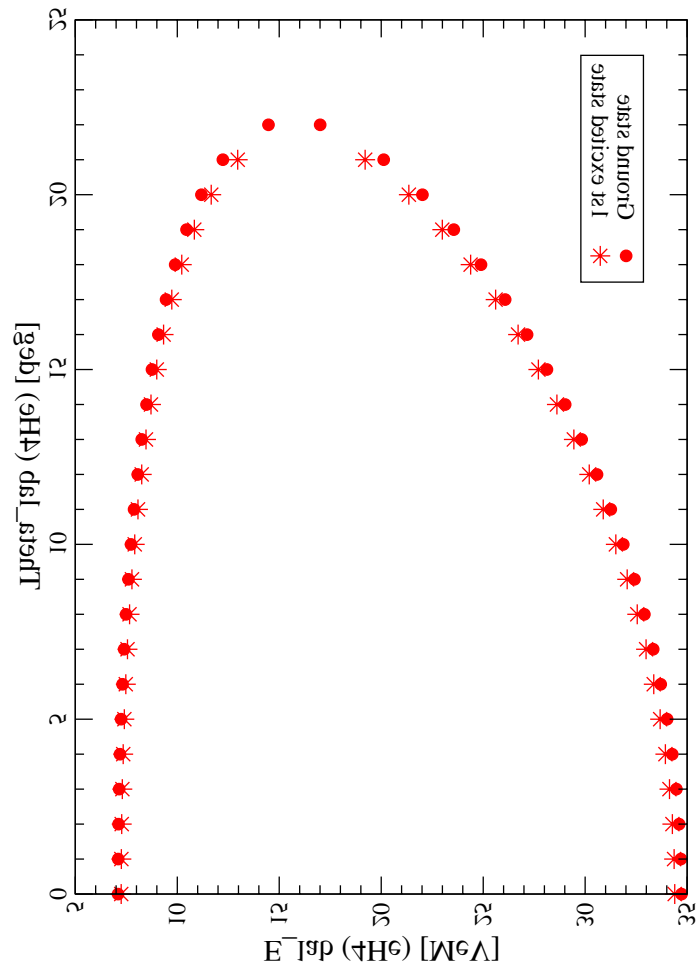
Difficulties: Kinematic shifts $dE/d\theta$

$^{22}\text{Ne}(p,\alpha)^{19}\text{F}$ @ $E=5$ MeV



- Low energies (no particle identification)
- use small detectors
- Coincidences very difficult

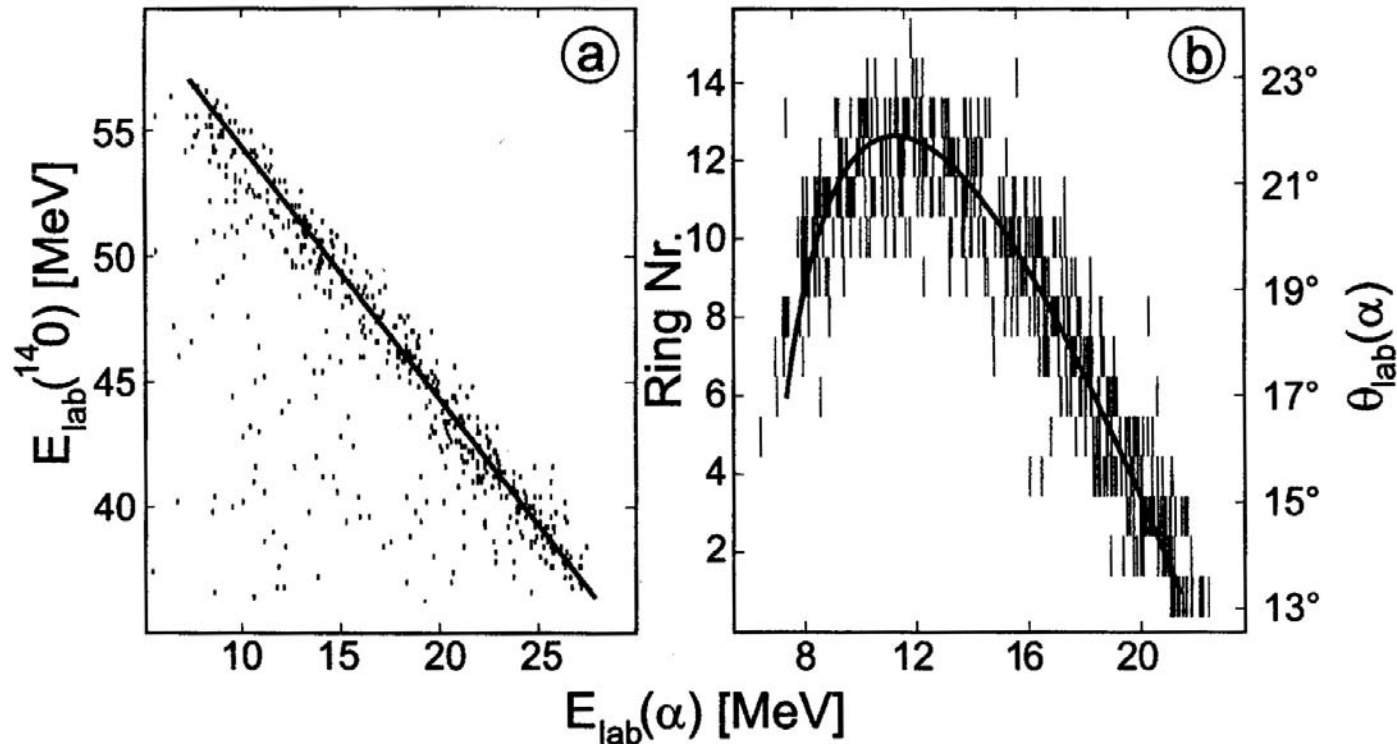
Inverse kinematics: detect both particles



- Difficult to get good angle definition
- Difficult to separate individual states

Inverse kinematics: detect both particles

Example: ${}^1\text{H}({}^{17}\text{F},\alpha){}^{14}\text{O}$



Angle uncertainty in close geometry!

Advantages/disadvantages of Si detectors

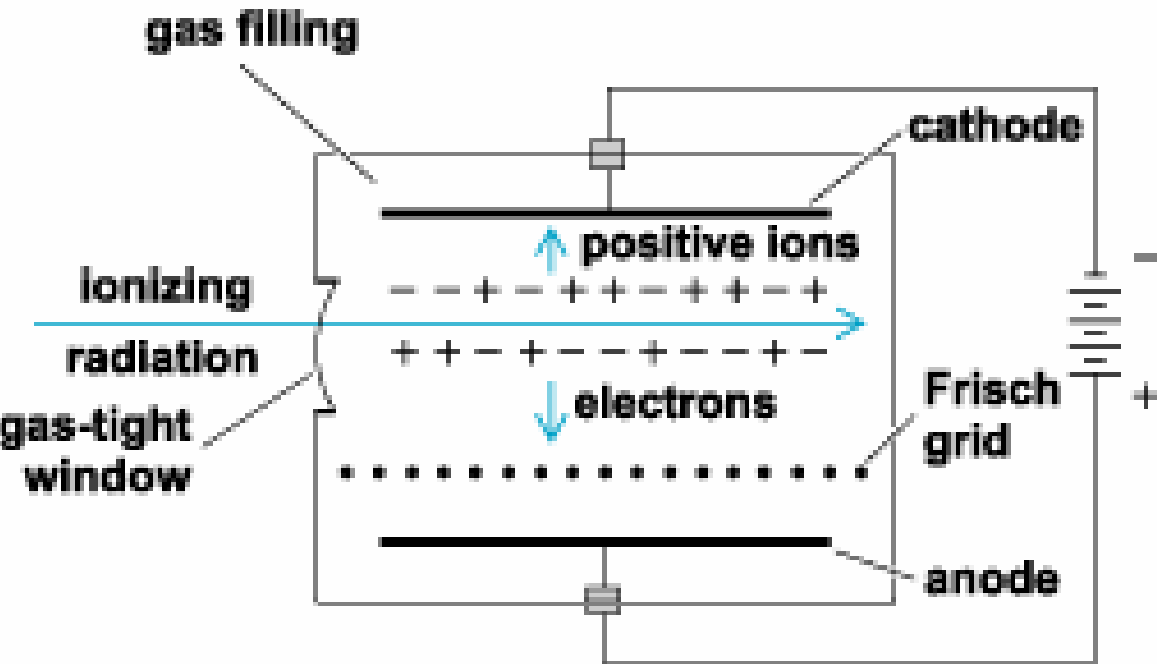
- + Commercially available
- + Compact
- + Good time resolution
- + Good count rate capabilities
- Expensive
- Easy to destroy
- difficult to produce thin and homogeneous.



Use a gas-filled ionization chamber

Ionization chambers

Types of ionization chambers:

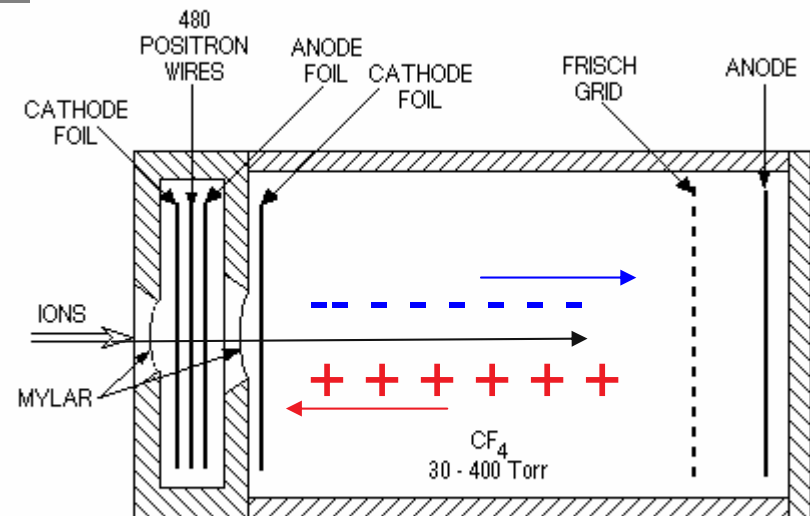


- + good Bragg peak
- + good range signal
- - long drift distance

BRAGG CURVE DETECTOR

Standard ionization chamber

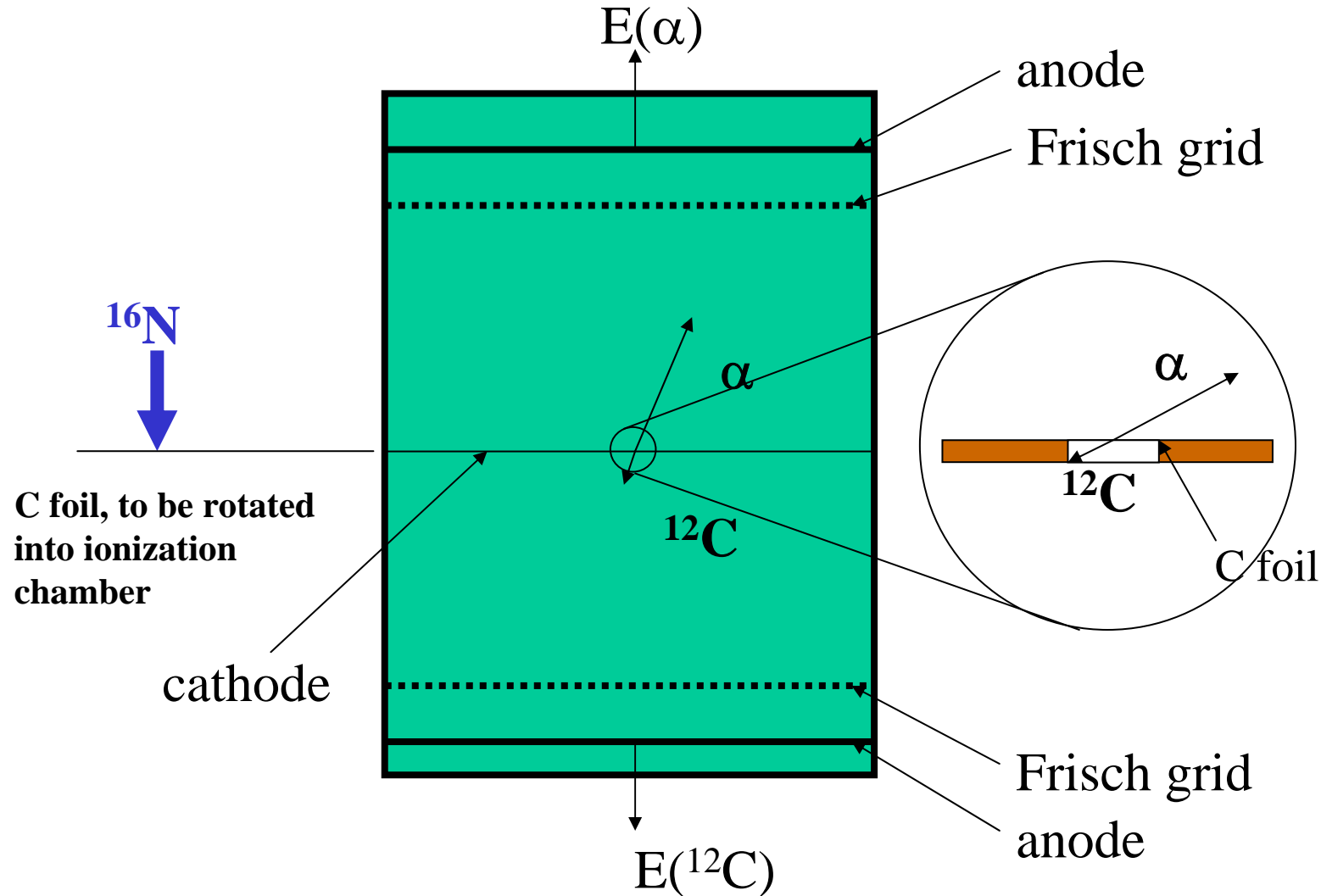
- + short drift distances
- + subdivided anode (ΔE)
- - inferior Z-separation



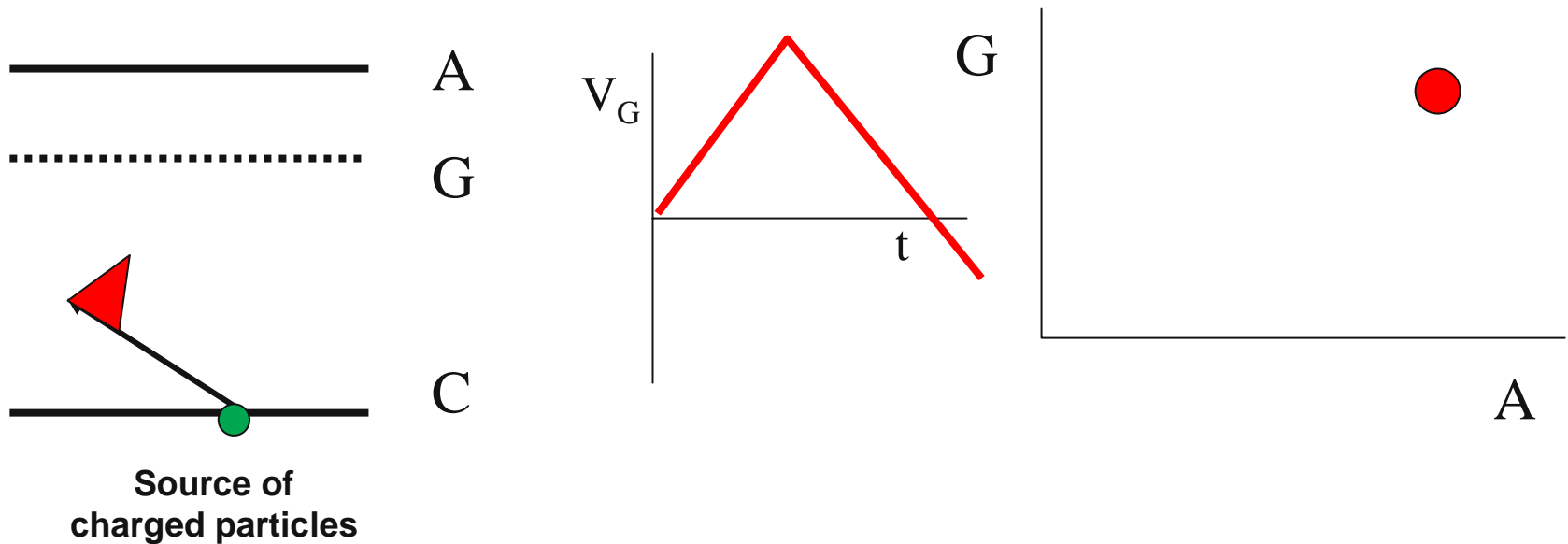
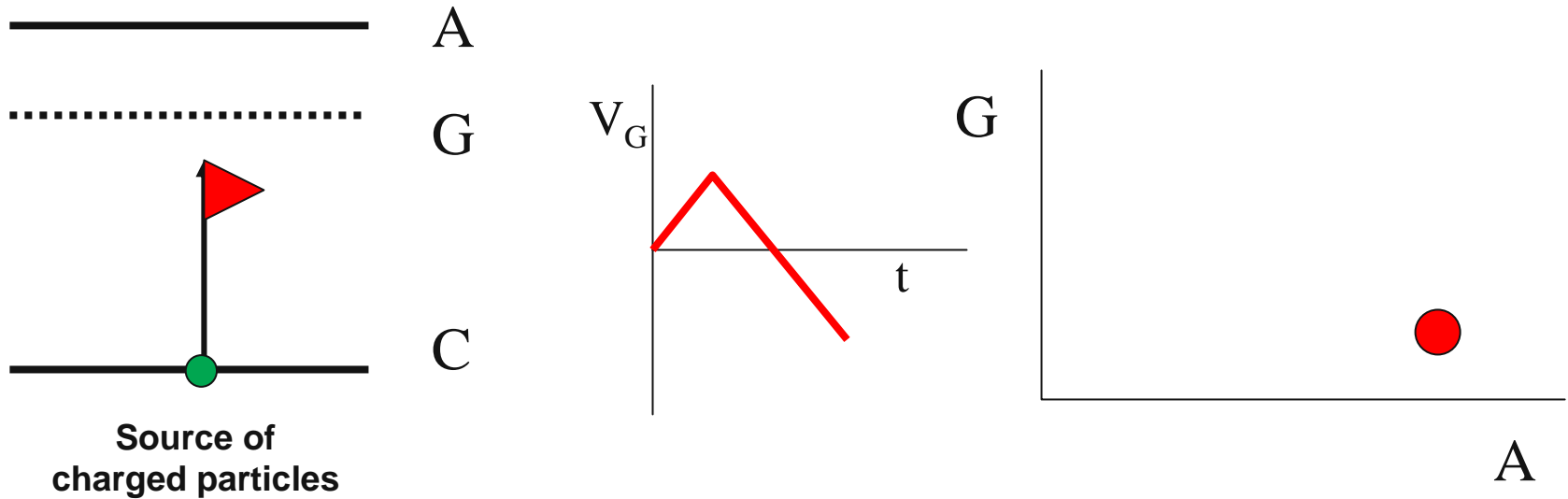
Cross section of Detector 1 available for the spectrographs.

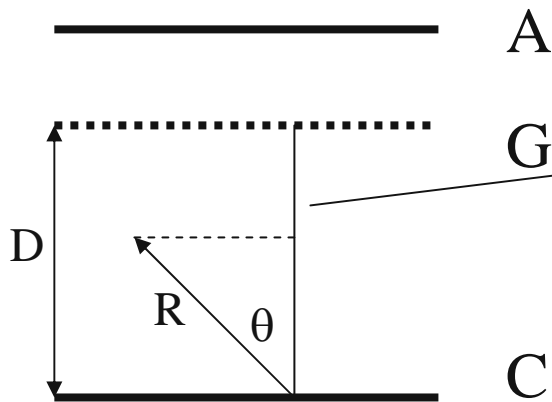
Some advanced ionization chambers

Twin-Ionization Chamber



Emission angle dependence of the Frisch grid signal





$$V_G \sim E \cdot (D - R \cos \theta)$$

$$V_G \sim E \cdot \left(1 - \lambda \frac{E^2}{mZ^2} \cos \theta \right)$$

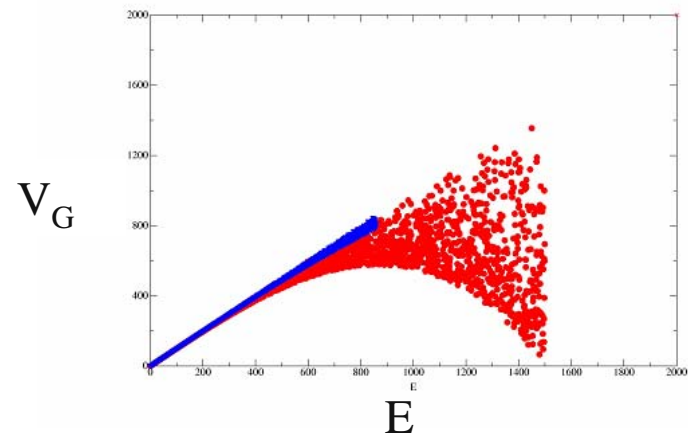
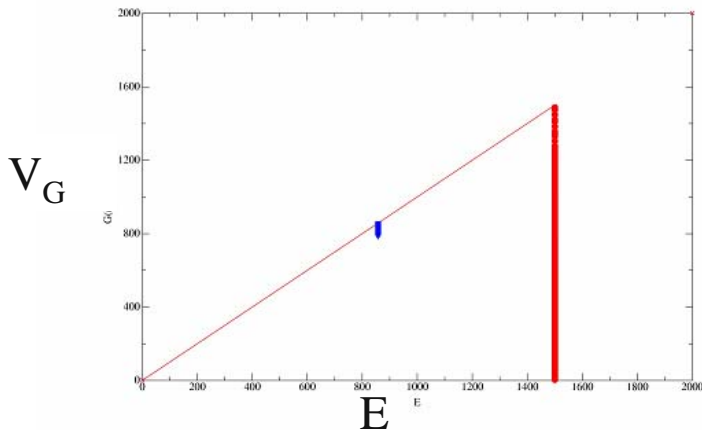
For $^{10}\text{B}(n, \alpha)^7\text{Li}$

$E_\alpha = 1.5 \text{ MeV}$, random θ

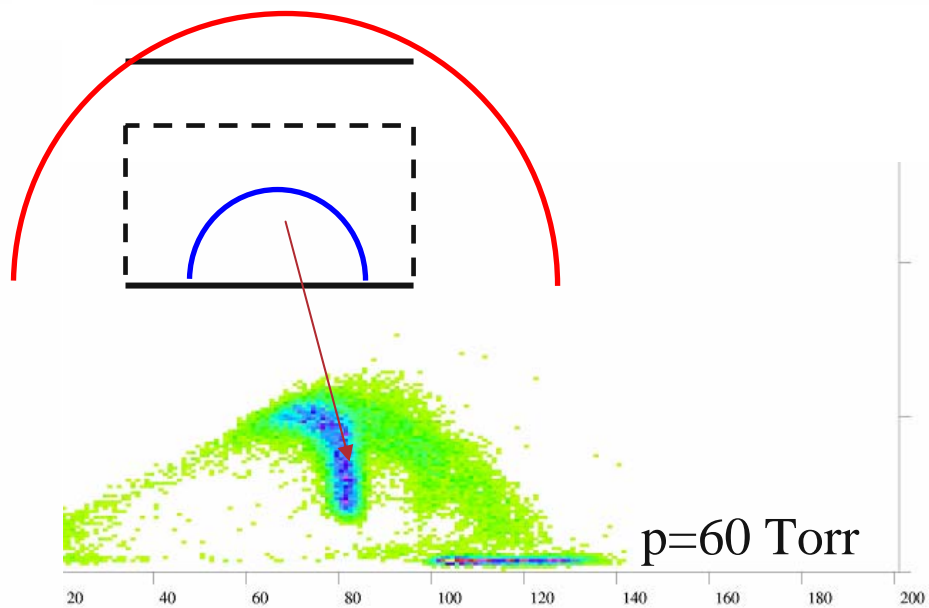
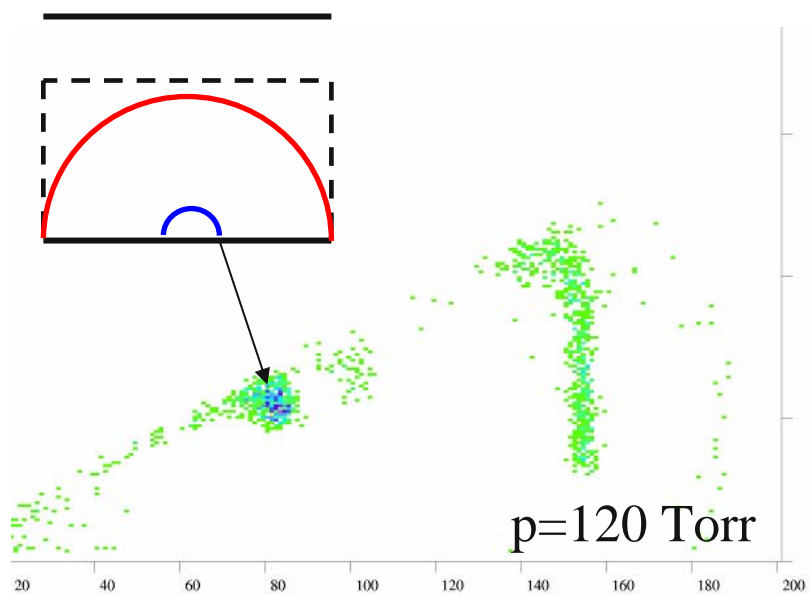
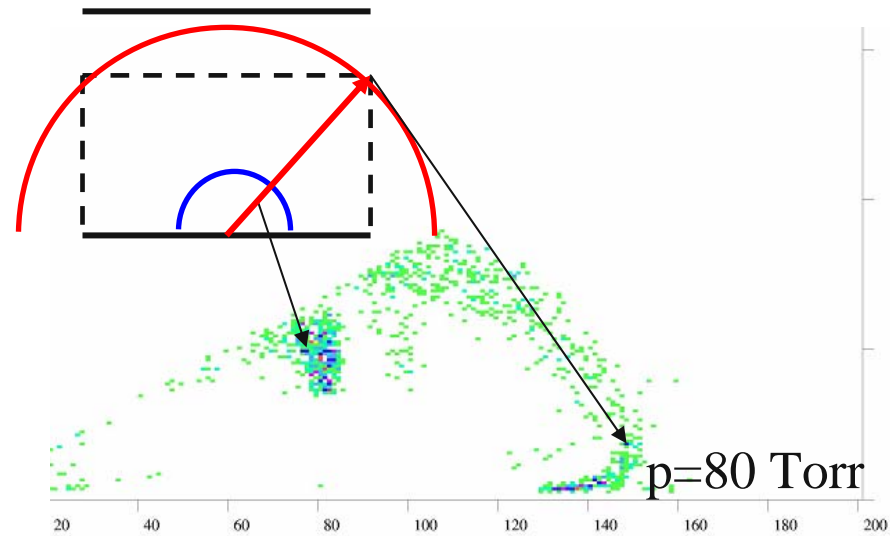
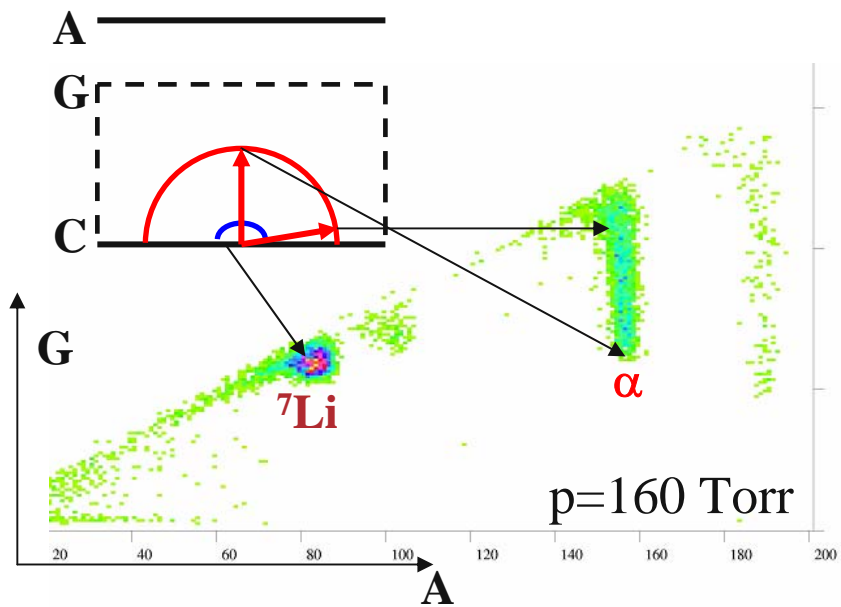
$E_{\text{Li}} = 4/7 * E_\alpha$

random E_α , random θ

$E_{\text{Li}} = 4/7 * E_\alpha$



Pressure dependence



Some comments about backgrounds:

Well-known for γ -detectors (e.g. ^{40}K)

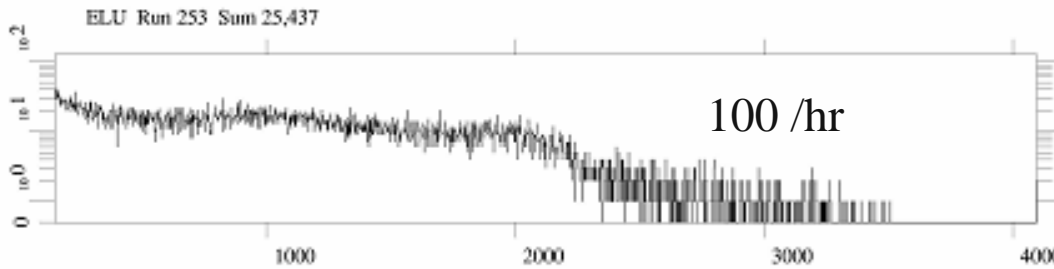
For particle detectors:

- Cosmic rays
- Radon/Uranium contamination in the counter material

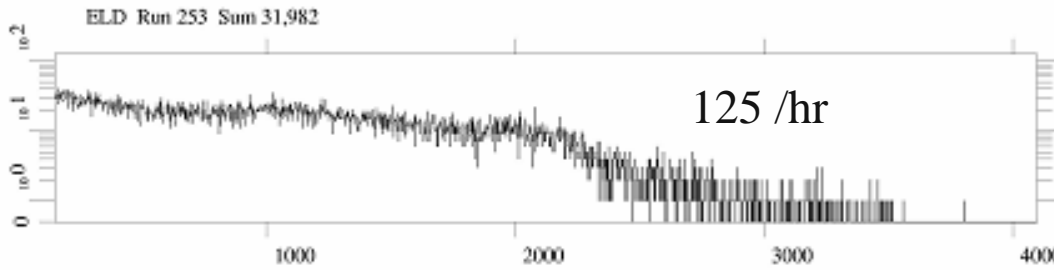
(see articles about low-background, underground experiments)

Background run – 0.925×10^6 s (257 hr)

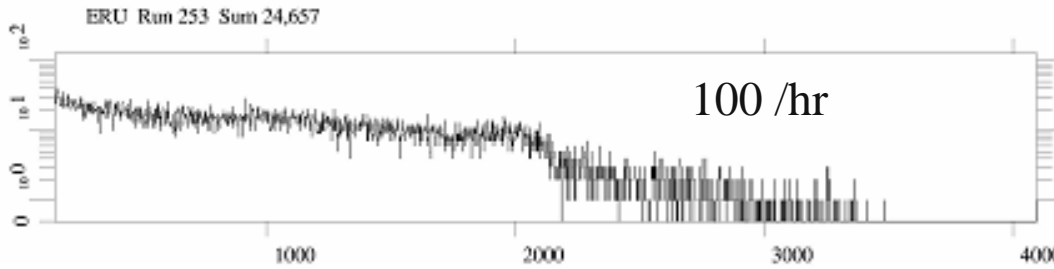
ELU



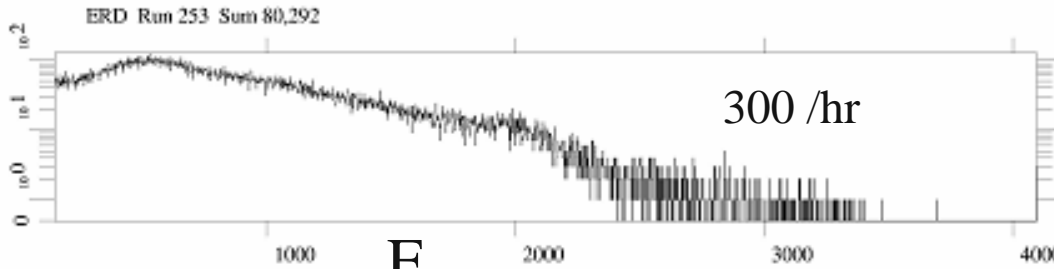
ELD



ERU

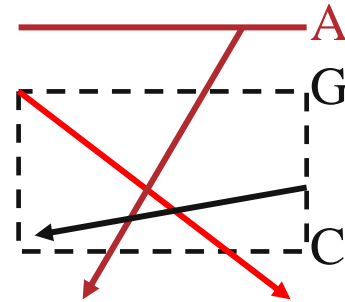


ERD



counts

E



Al: 16/hr

SS: 12/hr

Solder: 240/hr

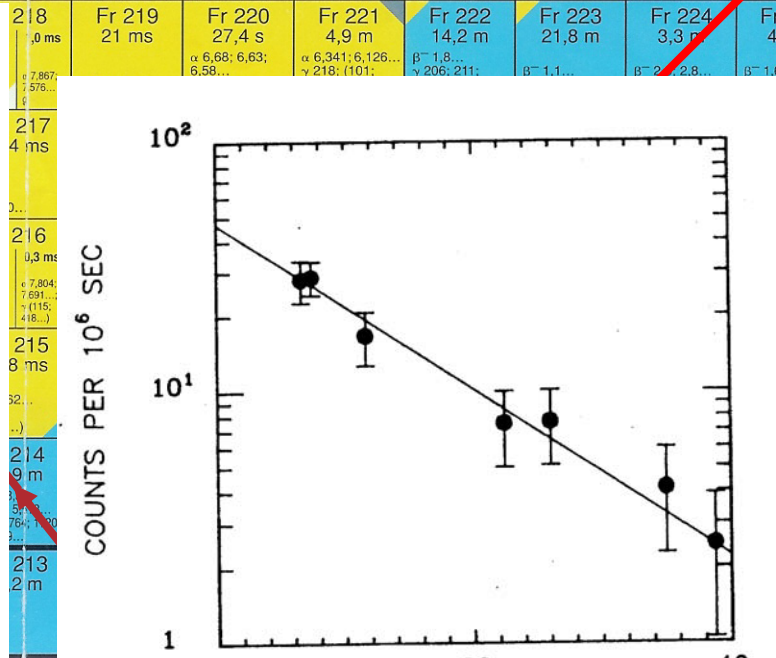
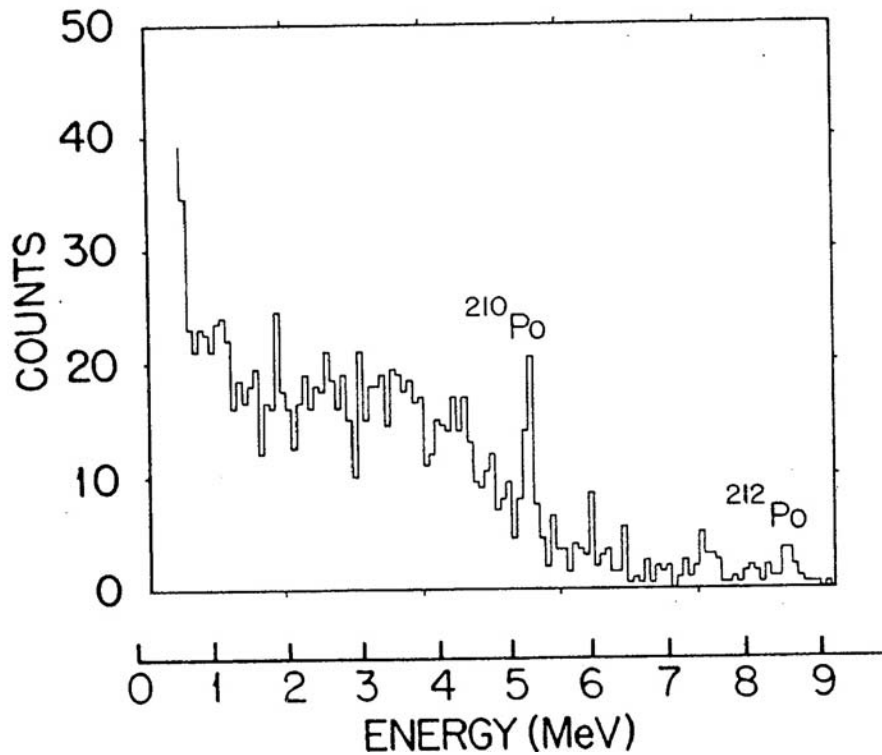
Background in double β decay

We have discovered a broad peak at 5.2 MeV with its leading edge at 5.3 MeV followed by a significant continuum. A similar peak has been observed in the UCSB-LBL detector³¹ at 5.1 MeV and has been attributed to a Doppler broadened line produced by the reaction $^{28}\text{Si}(n,n\gamma)^{28}\text{Si}$. We have been successful in reproducing our line at 5.2 MeV in a simple laboratory experiment. When soft solder is melted, the ^{210}Po , from the sequential decays of ^{210}Pb and ^{210}Bi , concentrates on the surface of the bead. After melting and solidifying several beads of solder, α spectra from their surfaces observed with a surface barrier detector were also found to contain this peak. The same phenomenon was observed in the UCI (University of California, Irvine) time projection chamber, and

T. Avignone et al. PRC 34,666(1986)

^{210}Po background

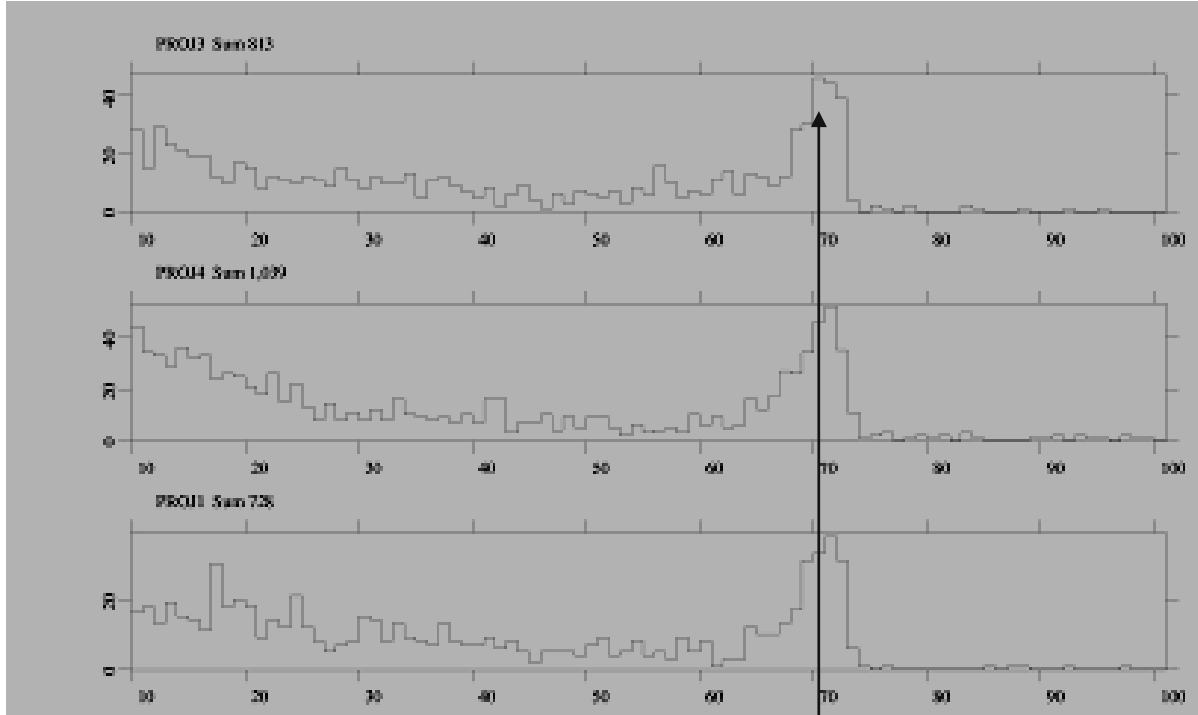
Ac 213 0,80 s α 7,36	Ac 214 8,2 s α 7,214; 7,082... ϵ	Ac 215 0,17 s α 7,604 ϵ	Ac 216 0,33 ms - 0,33 ms α 9,028; 9,106... α 9,07; 8,99	Ac 217 0,74 μs - 69 ns γ 660; 486; 382... α 10,54... α 9,65	Ac 218 1,1 μs α 9,205 α 8,664	Ac 219 11,8 μs α 8,664	Ac 220 26 ms α 7,85; 7,91; 7,68... γ 134...	Ac 221 52 ms α 7,65; 7,44; 7,38...	Ac 222 63 s - 5,0 s α 6,81; 6,75; 6,99; 7,00... γ 7; ... α 7,009; 6,963	Ac 223 2,10 m α 6,647; 6,662; 6,564... γ (99; 191; 84...)	Ac 224 2,9 h ϵ α 5,142; 6,060; 6,214... γ 216; 132	Ac 225 10,0 d α 5,830; 5,793; 5,732... γ 100; (150; 188; 63...); ϵ	Ac 226 29 h β^- 0,9; 1,1 α ; α 5,34 γ 230; 158; 254; 186...	Ac 227 β^- 0,0 α 4,9 γ (100; 880)
Ra 212 13 s α 6,9006 ϵ ?	Ra 213 2,1 ms - 2,74 m α 6,624; 1063; 161... α 8,466; 8,357... α 6,521... α 7,110; 215... ϵ	Ra 214 2,46 s α 7,136 ϵ	Ra 215 1,6 ms α 8,699... α 8,699...	Ra 216 2,0 ns - 0,18 μs γ 580; 476; 344... α 9,591; 11,020... α 9,349	Ra 217 1,6 μs α 8,99	Ra 218 25,6 μs α 8,39 α 8,39 α 8,39	Ra 219 10 ns α 7,679; 7,989... γ 316; 214; 592...	Ra 220 23 ms α 7,46... α 7,46...	Ra 221 28 s α 6,613; 6,761; 6,668... γ 149; 93; 174... α 6,613; 6,761; 6,668... γ 149; 93; 174... α 6,613; 6,761; 6,668... γ 149; 93; 174...	Ra 222 38 s α 6,559; 6,237... γ 324; (329; 473...) α 6,559; 6,237... γ 324; (329; 473...)	Ra 223 11,43 d α 5,7162; 5,6087... γ 269; 154; 324... α 5,7162; 5,6087... γ 269; 154; 324... α 5,7162; 5,6087... γ 269; 154; 324...	Ra 224 3,66 d α 5,6854; 5,4486... γ 241...; α 12,0 α 5,6854; 5,4486... γ 241...; α 12,0	Ra 225 14,8 d β^- 0,3; 0,4 γ 40 ϵ	Ra 226 16 d α 4,78 γ 186; 83 α < 0
Fr 218 0,0 ms α 7,867; 7,576... α 7,867; 7,576... α 7,867; 7,576...	Fr 219 21 ms α 6,68; 6,63; 6,58...	Fr 220 27,4 s α 6,68; 6,63; 6,58...	Fr 221 4,9 m α 6,341; 6,126... β^- 1,8... α 6,341; 6,126... β^- 1,8...	Fr 222 14,2 m β^- 1,8... α 6,341; 6,126... β^- 1,8...	Fr 223 12,8 m β^- 1,1... α 6,341; 6,126... β^- 1,1...	Fr 224 3,3 m β^- 2,2... α 6,341; 6,126... β^- 2,2...	Fr 225 4 m β^- 1,4... α 6,341; 6,126... β^- 1,4...							



Alpha background (2.5×10^4 s)

P=760 Torr

ELU



130/hr

ELD

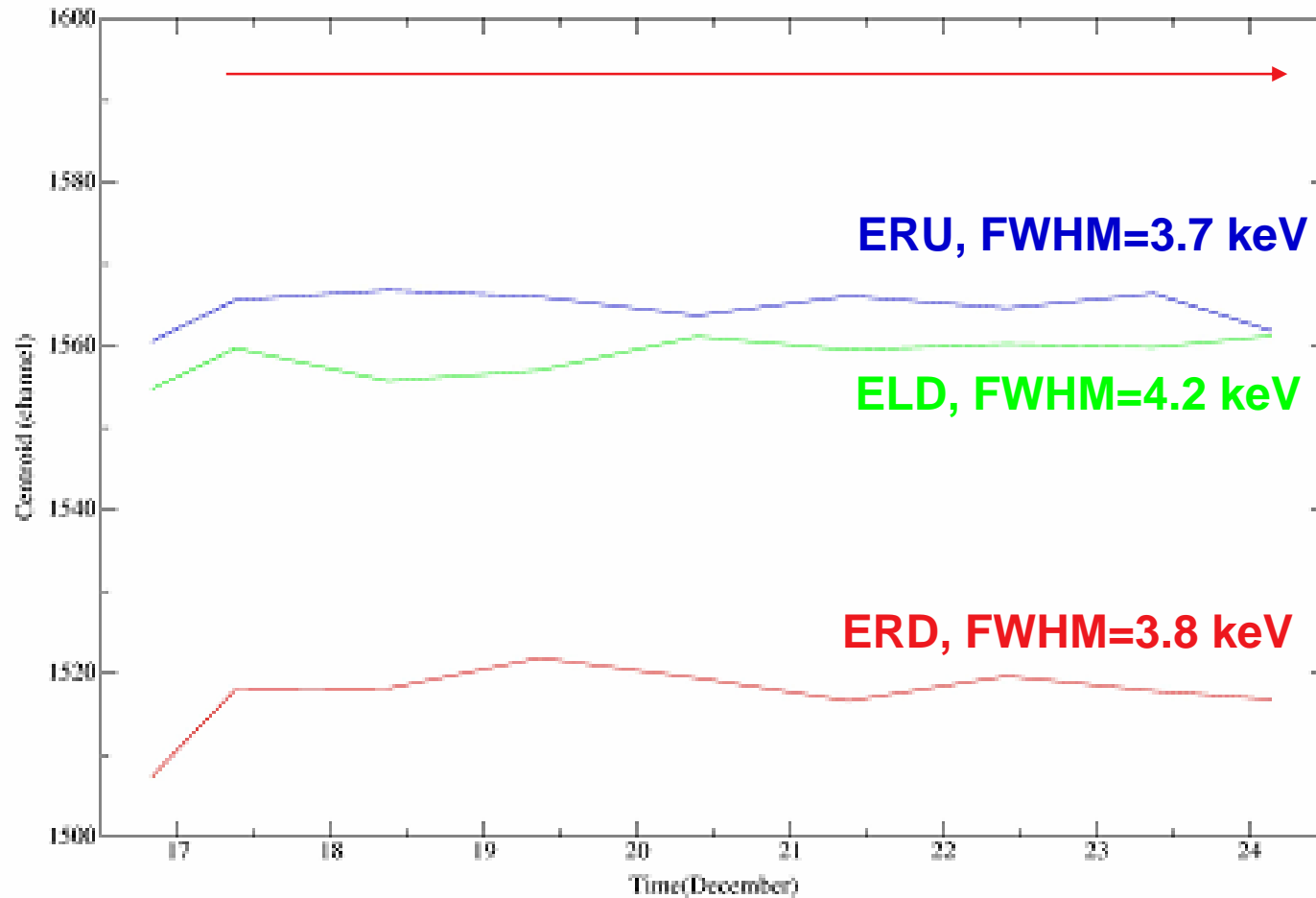
170/hr

ERU

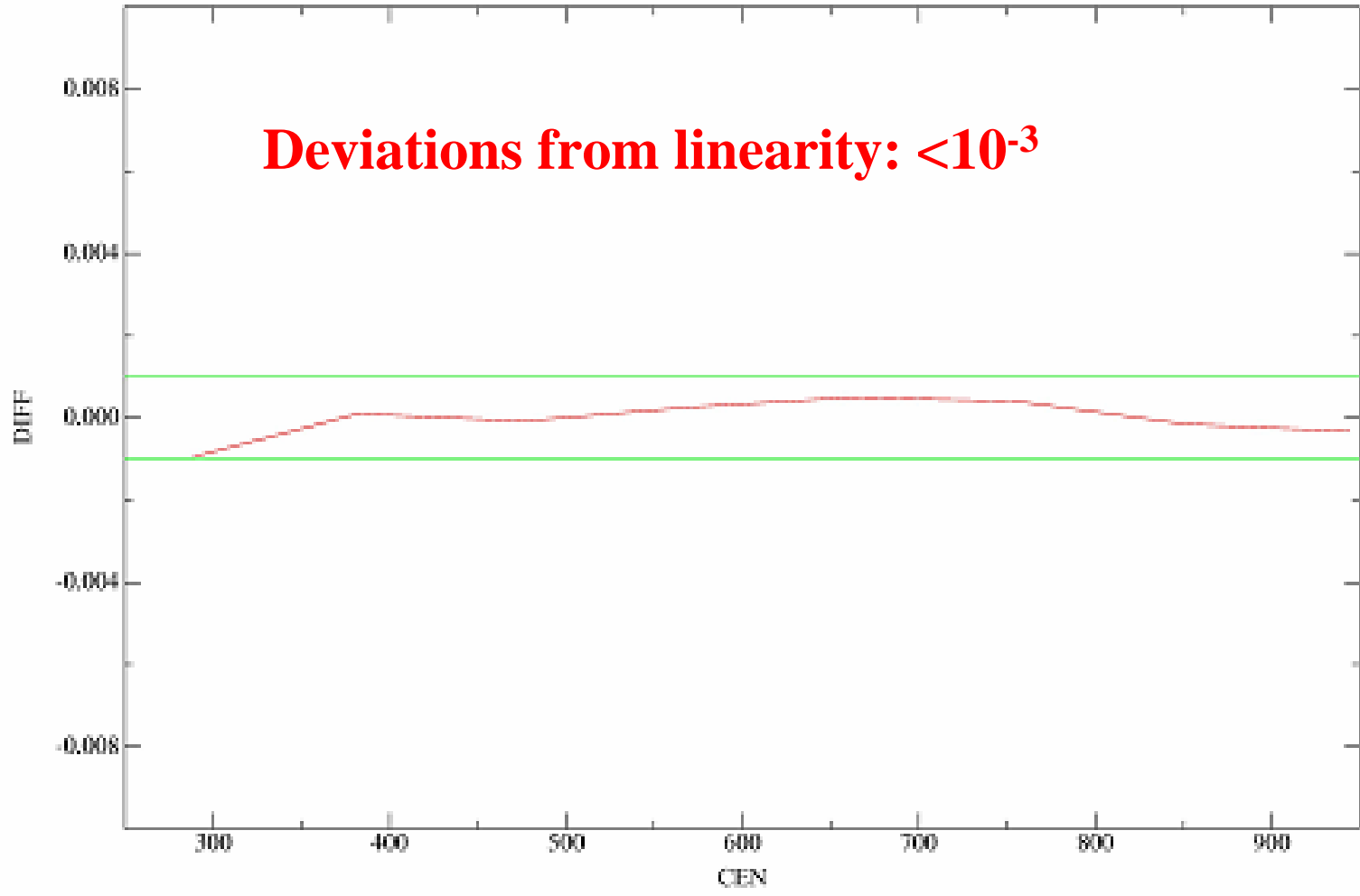
110/hr

~ 5.2 MeV

Long-time stability of ionization chambers



Deviations from linearity: $<10^{-3}$



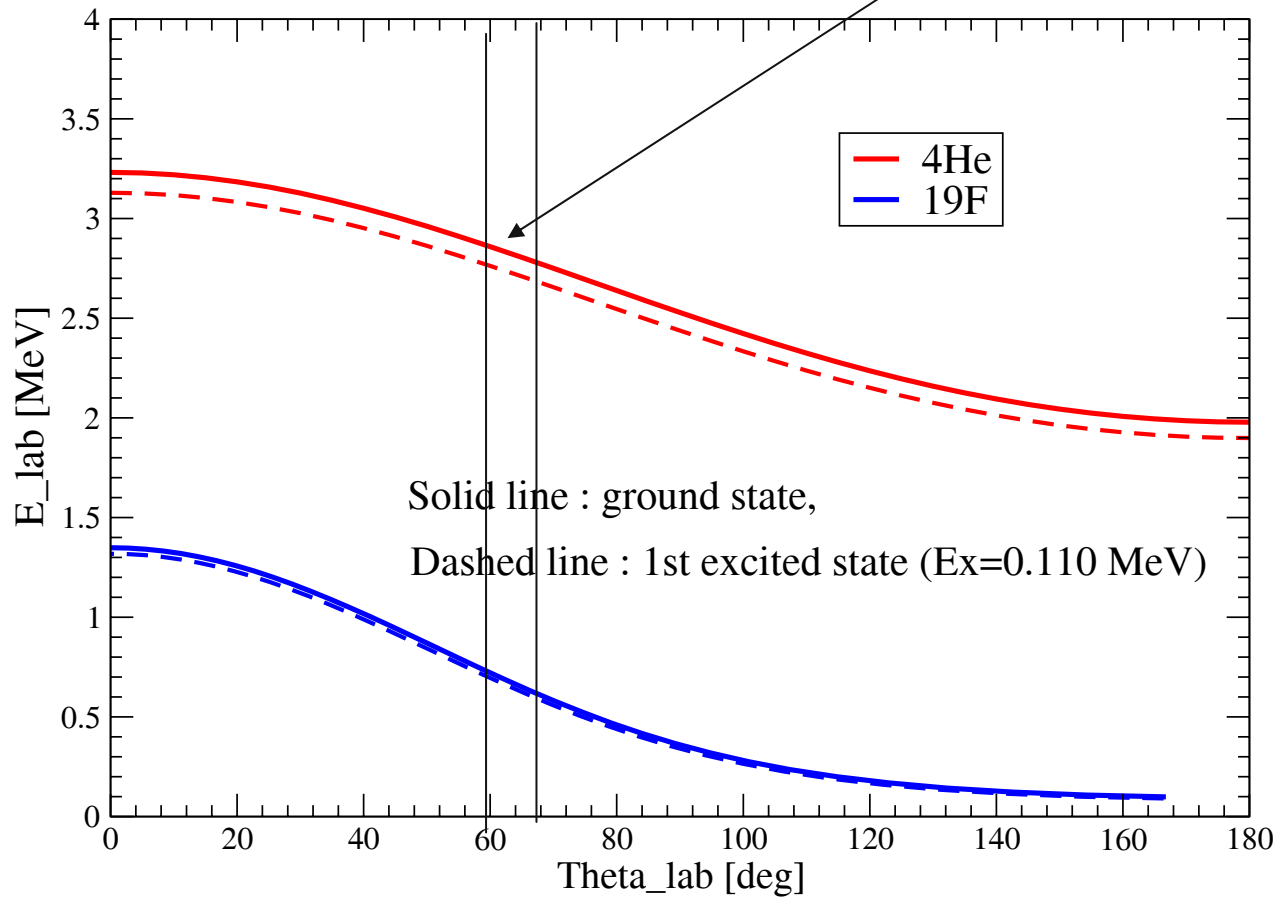
Advantages/disadvantages of ionization chambers

- + can be optimized for application
- + available in large sizes
- + can be built very thin and homogeneous
- + good energy resolution and stable
- + inexpensive
- + hard to destroy
- - poor time resolution (add timing detector)
- - need good entrance foils (see next lecture)
- - choose special Pb-free solder

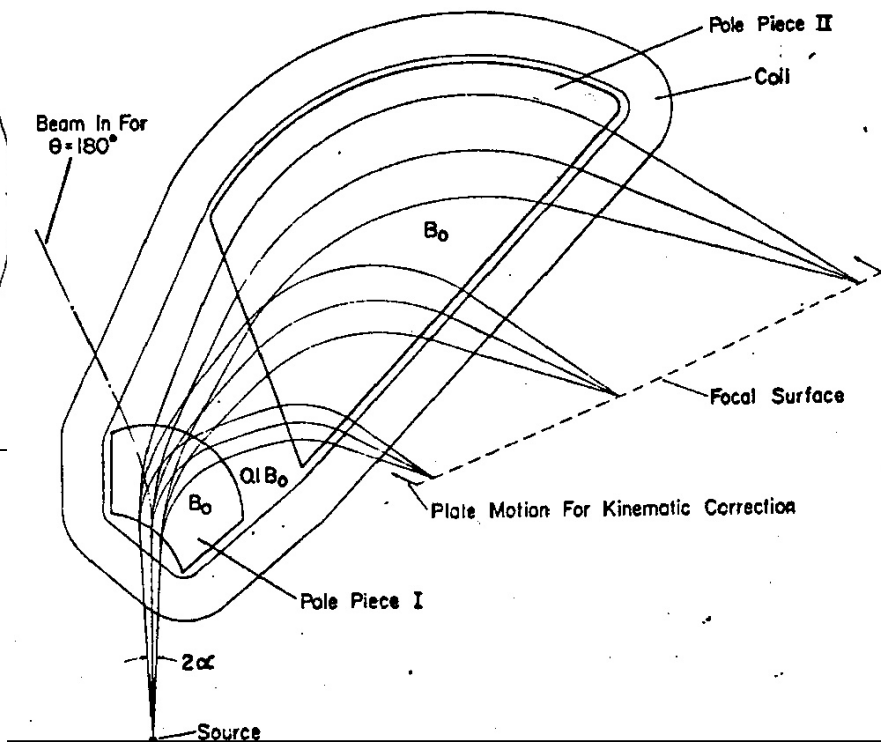
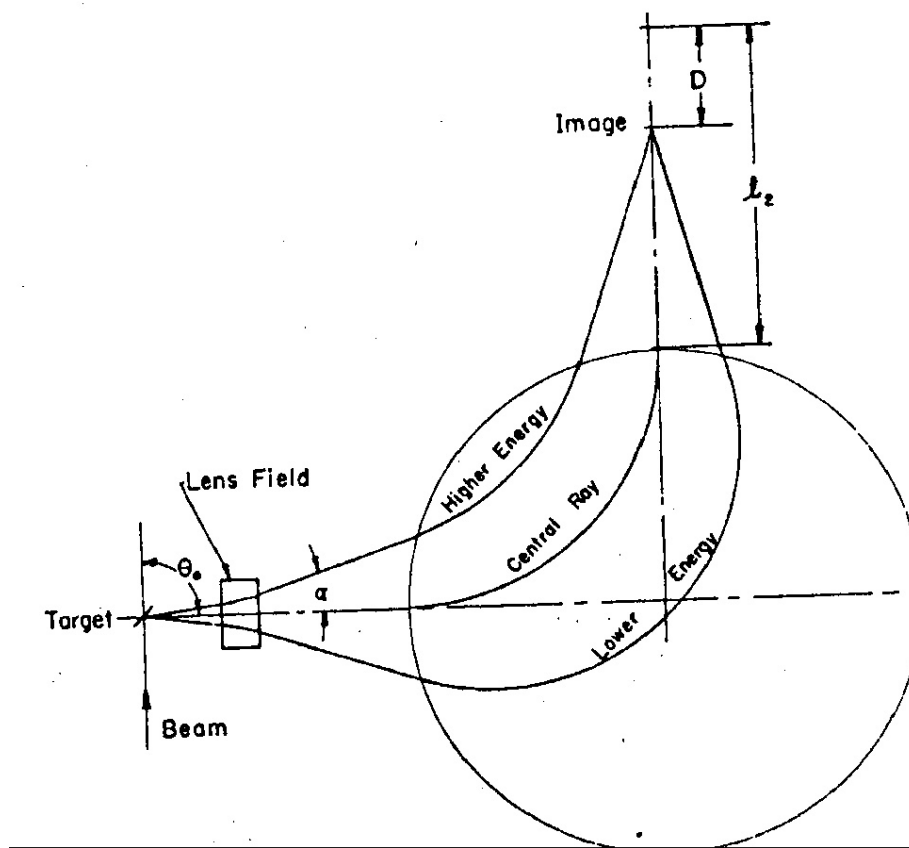
Magnetic Spectrographs

Compensating the kinematic shift $dE/d\theta$

$^{22}\text{Ne}(p,a)^{19}\text{F}$ @ $E=5$ MeV



Compensating the kinematic shift in a magnetic spectrometer



Large Acceptance Spectrometers – Recent Examples:

(identification of exotic nuclei, coincidence studies)



MAGNEX (Catania)



PRISMA (Legnaro)



VAMOS (GANIL)

$\Omega < 100 \text{ msr}$

Advantages/disadvantages of magnetic spectrometers

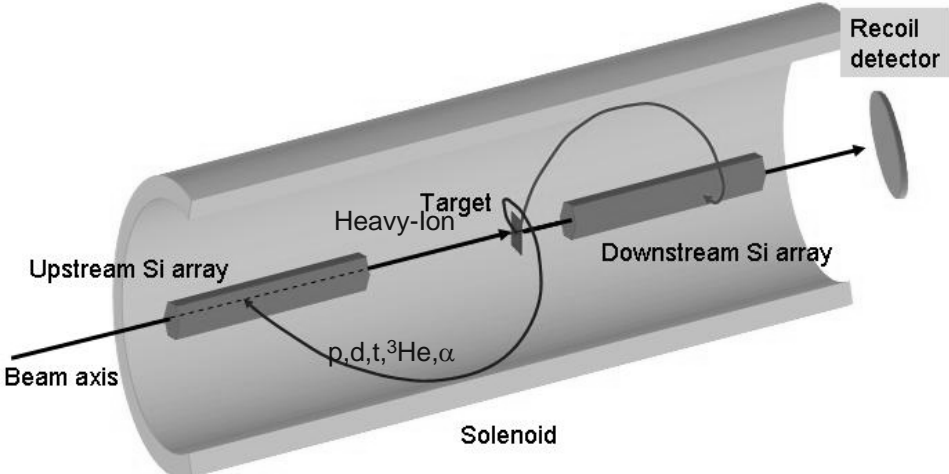
- + can compensate for kinematic shifts
- + best energy resolution
- + good count rate capabilities
- + good particle separation (m and Z)
(see lecture II)
- - large and expensive
- - small solid angle (< 100 msr)

HELIOS spectrometer , a new spectrometer for 'inverse reactions'

Inverse kinematics

Measured quantities
 Flight time: $T_{\text{flight}} = T_{\text{cyc}}$
 Position: Z
 Energy: E_{lab}

Derived quantities
 Part. ID: m/q
 Energy: E_{cm}
 Angle: θ_{cm}



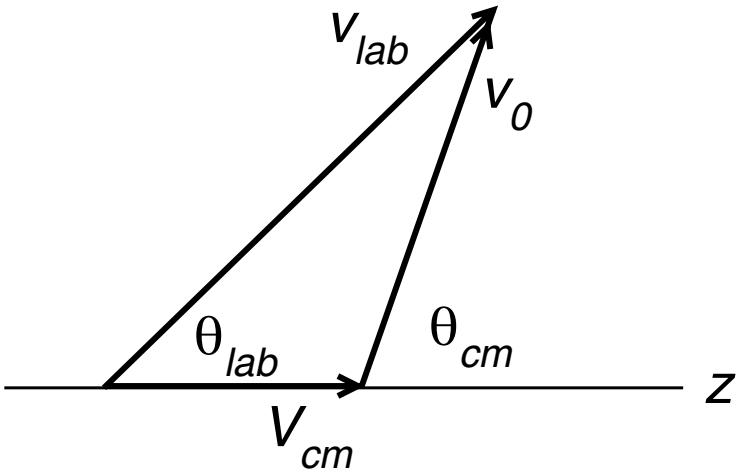
Field: 3 Tesla	
Particle	T_{cyc} (ns)
p	21.8
d, α	43.6
t	65.7
^3He	32.8

$$\frac{m}{q} = \frac{eB}{2\pi} \times T_{\text{flight}}$$

$$E_{\text{cm}} = E_{\text{lab}} + \frac{1}{2} m V_{\text{cm}}^2 - \frac{V_{\text{cm}} q e B Z}{2\pi}$$

$$\theta_{\text{cm}} = \arccos \left(\frac{1}{2\pi} \frac{q e B Z - 2\pi m V_{\text{cm}}}{\sqrt{2m E_{\text{lab}} + m^2 V_{\text{cm}}^2 - m V_{\text{cm}} q e B Z / \pi}} \right)$$

Simple kinematics



$$z = v_{\parallel} T_{cyc} = (V_{cm} + v_0 \cos \theta_{cm}) T_{cyc}$$

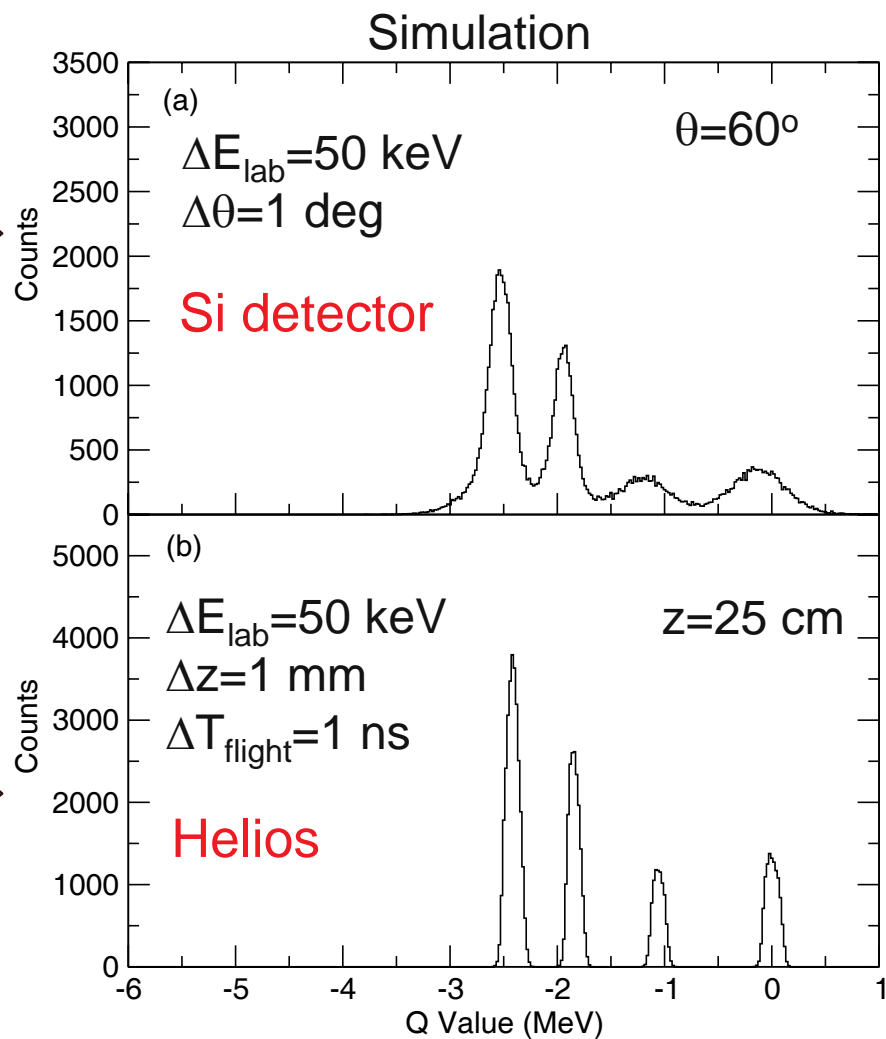
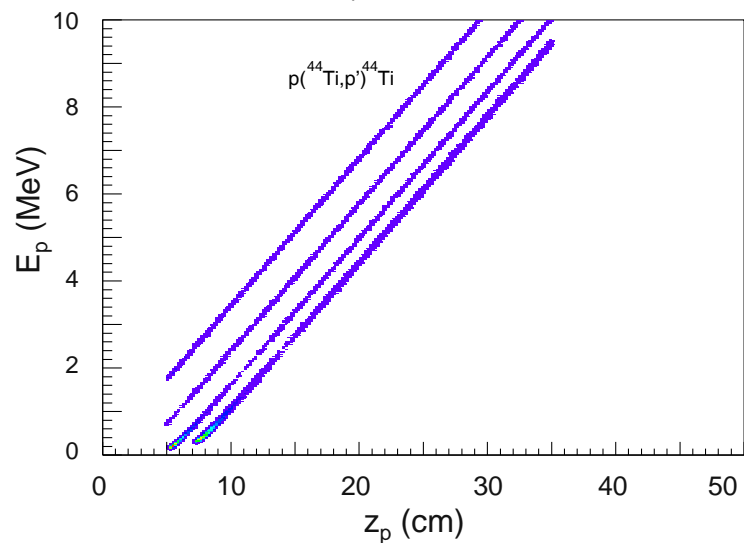
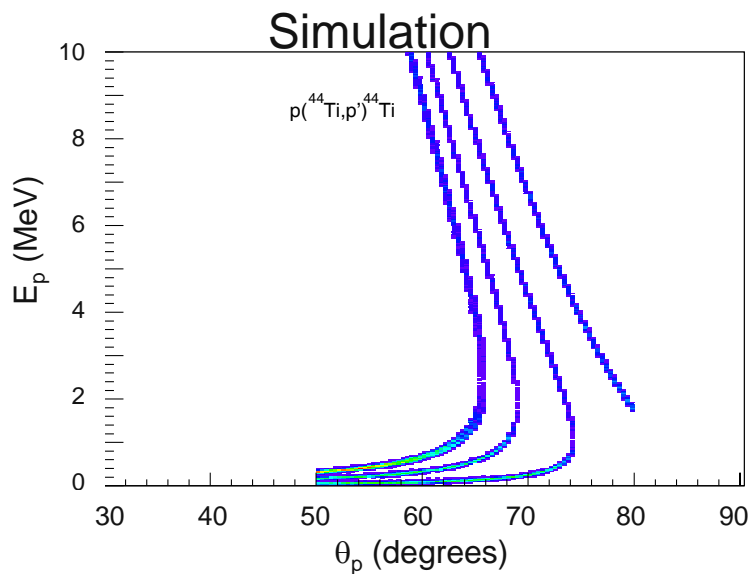
$$\Rightarrow v_0 \cos \theta_{cm} = \frac{z}{T_{cyc}} - V_{cm}$$

$$E_{lab} = \frac{m}{2} [v_{\parallel}^2 + v_{\perp}^2] = \frac{m}{2} [(v_0 \cos \theta_{cm} + V_{cm})^2 + v_0^2 \sin^2 \theta_{cm}]$$

$$= \frac{m}{2} [v_0^2 \cos^2 \theta_{cm} + V_{cm}^2 + 2v_0 V_{cm} \cos \theta_{cm} + v_0^2 \sin^2 \theta_{cm}]$$

$$= E_{cm} - \frac{m}{2} V_{cm}^2 + \frac{m V_{cm} z}{T_{cyc}}$$

$p(^{44}\text{Ti}, p')^{44}\text{Ti}$ kinematics



High Efficiency Spectrometers



**Superconducting Solenoid
(Transfer Reactions
in inverse
Kinematics)**

$^{132}\text{Sn}(d,p)^{133}\text{Sn}$ kinematics

